Coordinatively Unsaturated Ruthenium Phosphine Half-Sandwich Complexes: Correlations to Structure and Reactivity

Halikhedkar Aneetha, Manuel Jiménez-Tenorio, M. Carmen Puerta, and Pedro Valerga*

Departamento de Ciencia de Materiales e Ingeniería Metalúrgica y Química Inorgánica, Facultad de Ciencias, Universidad de Cádiz, 11510 Puerto Real, Cádiz, Spain

Valentin N. Sapunov, Roland Schmid, and Karl Kirchner

Institute of Applied Synthetic Chemistry, Vienna University of Technology, Getreidemarkt 9/153, A-1060 Vienna, Austria

Kurt Mereiter

Institute of Chemical Technologies and Analytics, Vienna University of Technology, Getreidemarkt 9, A-1060 Vienna, Austria

Received May 6, 2002

A number of 16e two-legged piano-stool complexes [Cp*Ru(PP)][BAr′$_4$] have been prepared by reaction of NaBAr′$_4$ with either [Cp*RuCl(PP)] (PP = $(PEt_3)_2$, $^iPr_2PCH_2CH_2P^iPr_2$ (dippe), $(PPh_3)_2$) or [Cp*RuCl(PR_3)] plus PR_3 (PR_3 = PMe^iPr_2, PPh^iPr_2) in fluorobenzene under argon. The complexes [Cp*Ru$(PEt_3)_2$][BAr′$_4$], [Cp*Ru(dippe)][BAr′$_4$], and [Cp*Ru$(PMe^iPr_2)_2$][BAr′$_4$] have been structurally characterized by X-ray crystallography. Attempts to isolate analogous species containing other phosphine ligands such as P^iPr_3, PCy_3, and PMe_3 led to the sandwich derivative [Cp*Ru(η^6-FPh)][BAr′$_4$], which was also structurally characterized. Both [Cp*Ru-$(PPh_3)_2$][BAr′$_4$] and [Cp*Ru$(PPh^iPr_2)_2$][BAr′$_4$] are unstable and rearrange to the 18e sandwich species [Cp*Ru(η^6-$C_6H_5PR_2$)][BAr′$_4$] and to [Cp*Ru(η^6-$C_6H_5POR_2$)][BAr′$_4$] (R = Ph, ^{i}Pr) under trace amounts of oxygen. The geometry of the 16e complexes as well as their affinity for an additional ligand depend on the substituents on the phosphorus. The reactivity with respect to the addition of N_2, PR_3, O_2, H_2, and HCl to form 18e derivatives has been studied. Some model systems have been analyzed using density functional theory (DFT) calculations. Also included are comparative studies on the NN counterparts. The moieties $[CpRu(PP)]^+$ (PP = $(PH_3)_2$, $H_2PCH_2CH_2PH_2$) adopt typically pyramidal structures (i.e. in the absence of bulky and rigid substituents on P) versus planar structures of $[CpRu(NN)]^+$ (NN = $(NH_3)_2$, H_2-$NCH_2CH_2NH_2$). $[CpRu(PP)]^+$ is more stable but has nevertheless a higher affinity of adding a σ ligand than $[Cp^*Ru(NN)]^+$.

Introduction

Half-sandwich d^6 complexes of the group 8 elements Fe, Ru, and Os, ubiquitous in organometallic chemistry, typically adhere to the 18e rule. There is, however, a small but growing number of relatively stable "genuine" 16e complexes.[1] Since such unsaturated compounds are potential catalysts, it is highly desirable to understand in more detail the parameters that are related to stability, reactivity, and structure. This goal will be achieved by the synergistic use of experiment and theory.

For the iron case, five unsaturated complexes of the type $[\eta^5$-Cp′Fe(PP)$]^+$ (Cp′ = Cp, Cp*, pentadienyl; PP = $Ph_2PCH_2CH_2PPh_2$ (dppe), $Pr^i_2PCH_2CH_2PPr^i_2$ (dippe), 2 PEt_3) have so far been isolated and structurally characterized.[2−4] All of them have a planar (C_{2v}) ground-state structure (i.e., the Cp plane is perpendicular to the P−Fe−P plane) and are paramagnetic (S = 1). These features are nicely reproduced by DFT calculations by Costuas and Saillard[5] in terms of both small HOMO−LUMO gap and weak HOMO−LUMO overlap (rendering the Jahn−Teller instability of the pseudo-C_{2v} geometry insignificant). It is interesting to note that, if a singlet ground state (S = 0) is assumed, the pyramidal structure would be favored. Furthermore, pyramidalization of the metal center is favored by strong π-acceptor ligands, especially if they are also strong σ-donors. Thus, with the weak π-acceptor phosphine ligands, the triplet state is the ground state, while with the strong π-acceptor CO ligand, the singlet state is more stable. The configurational stability of pyramidal vs planar 16e complexes depending on the electronic

(1) Poli, R. *Chem. Rev.* **1996**, *96*, 2135.

(2) Hamon, P.; Toupet, L.; Hamon, J.-R.; Lapinte, C. *Organometallics* **1996**, *15*, 10.

(3) de la Jara Leal, A.; Tenorio, M. J.; Puerta, M. C.; Valerga, P. *Organometallics* **1995**, *14*, 3839.

(4) Bleeke, J. R.; Wittenbrink, R. J.; Clayton, T. W., Jr.; Chiang, M. Y. *J. Am. Chem. Soc.* **1990**, *112*, 6539.

(5) Costuas, K.; Saillard, J.-Y. *Organometallics* **1999**, *18*, 2505.

10.1021/om020359r CCC: $22.00
Publication on Web 10/26/2002

properties of the ligands for diamagnetic systems has been analyzed in detail by the Hofmann[6] and Eisenstein[7] groups. As a result, the relative stability of the above iron complexes may be traced to the energetically unfavorable change in spin state, preventing the unsaturated complex from adding nucleophiles. This point of view has been put forward by Poli.[1] An unusual case of a neutral 14e half-sandwich complex, [Cp*Fe{N(SiMe$_3$)$_2$}], adopting a so-called "pogo-stick" structure, has been reported recently by Siemeling.[8] The solid-state structure of the diamagnetic complex is unprecedented in the chemistry of open-shell organometallics.

For the Ru situation, spin state arguments are not particularly relevant, owing to the larger HOMO−LUMO gap compared to that in the iron congeners. The stability of open-shell Ru complexes is enhanced on using strong π-donor ligands X, as in [Cp*Ru(PR$_3$)X] (R = Cy, ^{i}Pr, ^{t}Bu, X = halide, alkoxide, amide)[9−14] or [Cp*Ru(carbene)X] (carbene = 1,3-R$_2$-imidazol-2-ylidenes).[15] A very recent example of a π-stabilized 16e complex is [Cp*Ru(RNCR′NR)] (R = ^{t}Bu, Cy), in which the amidinate ligand is acting both as a σ- and π-donor to avoid unsaturation.[16]

In the course of our efforts to synthesize and characterize coordinatively unsaturated ruthenium complexes, we recently switched over to hard nitrogen donors. In this way the first genuine cationic 16e ruthenium complexes [Cp*Ru(Me$_2$NCH$_2$CH$_2$NR$_2$)]$^+$ (R = Me, ^{i}Bu)[17] and [CpRu(Me$_2$NCH$_2$CH$_2$NMe$_2$)]$^+$[18] became available. The nearly C_{2v} symmetric complexes are remarkably stable, particularly those of Cp*, and show surprisingly little affinity toward the simple ligands N_2, H_2, and ethylene despite the absence of π-donor stabilization, bulky ligands,[19] and spin state changes. Analogous [(η^5-Cp′)Ru(PP)]$^+$ complexes remain unknown so far, being obviously too reactive to be isolated. Such species, when generated in situ by halide (X) abstraction from the halide complex [(η^5-Cp′)Ru(PP)X], react readily with any suitable source of electrons to achieve the 18e configuration, be it solvent molecules, the counterion of the cationic complex, or even dinitrogen. The introduction of a salt of the bulky, noncoordinating anion [BAr′$_4$]$^-$ (Ar′ = 3,5-(CF$_3$)$_2$C$_6$H$_3$))[20] and its use as a halide scavenger in combination with fluorobenzene as the solvent open up new possibilities to generate and stabilize cationic, highly electrophilic, coordinatively unsaturated species. An example is the successful isolation of [(η^5-Cp′)Ru(NN)][BAr′$_4$].[17,18] However, the resulting 16e species generated in this way are potentially so reactive so as to scavenge trace amounts of dinitrogen present even in high-purity argon, giving dinitrogen-bridged complexes. This is what happens in the course of the reaction of [CpRu(P)$_2$Cl] ((P)$_2$ = dippe, (PEt$_3$)$_2$, (PMe^{i}Pr$_2$)$_2$) with NaBAr′$_4$ in fluorobenzene under argon, which yields [{CpRu(P)$_2$}$_2$(μ-N$_2$)][BAr′$_4$]$_2$.[21] Alternatively, familiar ligands such as PPh$_3$ may be forced to adopt a rare η^3-coordination mode, allowing the metal to attain the 18e configuration in [CpRu(η^3-PPh$_3$)(PMe^{i}Pr$_2$)][BAr′$_4$].[21]

We have found that halide abstraction from certain Cp*Ru complexes containing bulky phosphines having good σ-electron-donor capabilities leads to cationic 16e species of the type [Cp*Ru(PP)]$^+$. Such species are amenable to isolation in high yields and were unequivocally characterized by spectral techniques and occasionally single-crystal X-ray structure analysis. The present paper describes the outcome of our efforts to synthesize and characterize a number of coordinatively unsaturated species [Cp*Ru(PP)][BAr′$_4$]. Furthermore, their structural and chemical properties will be compared with theoretical treatments using density functional theory (DFT). Specifically, we compare the electronic structures of coordinatively unsaturated half-sandwich ruthenium complexes containing N and P donor coligands and their reactivities toward simple ligands. Part of the work has appeared as a preliminary communication.[22]

Experimental Section

All synthetic operations were performed under a dry argon atmosphere, using conventional Schlenk techniques. Tetrahydrofuran, diethyl ether, and petroleum ether (boiling point range 40−60 °C) were distilled from the appropriate drying agents. All solvents were deoxygenated immediately before use. The complexes [Cp*RuCl(PR$_3$)$_2$] (R = Et, Ph, Me),[23,24] [Cp*RuCl(dippe)],[25] and [Cp*RuCl(PR$_3$)] (PR$_3$ = PMe^{i}Pr$_2$, PPh^{i}Pr$_2$, P^{i}Pr$_3$, PCy$_3$)[9,11,13,26] as well as Na[BAr′$_4$][20] were prepared according to reported procedures. IR spectra were recorded in Nujol mulls on a Perkin-Elmer FTIR Spectrum 1000 spectrophotometer. UV−vis spectra were measured on a Milton Roy Spectronic 3000 Diode Array instrument. NMR spectra were taken on a Varian Unity 400 MHz or Varian Gemini 200 MHz instrument at 298 K unless otherwise stated. Chemical shifts are given in ppm from SiMe$_4$ (^{1}H and ^{13}C{^{1}H}) or 85% H$_3$PO$_4$ (^{31}P{^{1}H}). Microanalysis were performed by the Serveis Científico-Tècnics, University of Barcelona.

(6) Ward, T. R.; Schafer, O.; Daul, C.; Hofmann, P. *Organometallics* **1997**, *16*, 3207.
(7) Johnson, T. J.; Folting, K.; Streib, W. E.; Martin, J. D.; Huffman, J. C.; Jackson, S. A.; Eisenstein, O.; Caulton, K. G. *Inorg. Chem.* **1995**, *34*, 488.
(8) Siemeling, U.; Vorfeld, U.; Neumann, B.; Stammler, H.-G. *Organometallics* **1998**, *17*, 483.
(9) Campion, B. K.; Heyn, R. H.; Tilley, T. D. *J. Chem. Soc., Chem. Commun.* **1988**, 278.
(10) (a) Kölle, U.; Kossakowski, J.; Raabe, G. *Angew. Chem., Int. Ed. Engl.* **1990**, *29*, 773. (b) Kölle, U.; Rietmann, C.; Raabe, G. *Organometallics* **1997**, *16*, 3273.
(11) Arliguie, T.; Border, C.; Chaudret, B.; Devillers, J.; Poilblanc, R. *Organometallics* **1989**, *8*, 1308.
(12) Lindner, E.; Haustein, M.; Mayer, H. A.; Gierling, K.; Fawzi, R.; Steinmann, M. *Organometallics* **1995**, *14*, 2246.
(13) (a) Johnson, T. J.; Huffman, J. C.; Caulton, K. G. *J. Am. Chem. Soc.* **1992**, *114*, 2725. (b) Bickford, C. C.; Johnson, T. J.; Davidson, E. R.; Caulton, K. G. *Inorg. Chem.* **1994**, *33*, 1080.
(14) Braun, T.; Laubender, M.; Gevert, O.; Werner, H. *Chem. Ber./Recl.* **1997**, *130*, 559.
(15) (a) Huang, J.; Schanz, H.-J.; Stevens, E. D.; Nolan, S. P. *Organometallics* **1999**, *18*, 2370. (b) Huang, J.; Stevens, E. D.; Nolan, S. P.; Petersen, J. L. *J. Am. Chem. Soc.* **1999**, *121*, 2674.
(16) Yamaguchi, Y.; Nagashima, H. *Organometallics* **2000**, *19*, 725.
(17) (a) Gemel, C.; Mereiter, K.; Schmid, R.; Kirchner, K. *Organometallics* **1997**, *16*, 5601. (b) Gemel, C.; Sapunov, V. N.; Mereiter, K.; Ferencic, M.; Schmid, R.; Kirchner, K. *Inorg. Chim. Acta* **1999**, *286*, 114.
(18) Gemel, C.; Huffman, J. C.; Caulton, K. G.; Mauthner, K.; Kirchner, K. *J. Organomet. Chem.* **2000**, *593−594*, 342.
(19) Caulton, K. G. *New J. Chem.*, **1994**, *18*, 25.
(20) Brookhart, M.; Grant, B.; Volpe, A. F., Jr. *Organometallics* **1992**, *11*, 3920.
(21) Aneetha, H.; Jimenez-Tenorio, M.; Puerta, M. C.; Valerga, P.; Mereiter, K. *Organometallics* **2002**, *21*, 628.
(22) Jiménez-Tenorio, M.; Puerta, M. C.; Valerga, P.; Mereiter, K. *J. Am. Chem. Soc.* **2000**, *122*, 11230.
(23) Coto, A.; Jiménez-Tenorio, M.; Puerta, M. C.; Valerga, P. *Organometallics* **1998**, *17*, 4392.
(24) Fagan, P. J.; Mahoney, W. S.; Calabrese, J. C.; Williams, I. D. *Organometallics* **1990**, *9*, 1843.
(25) de los Ríos, I.; Jiménez-Tenorio, M.; Padilla, J.; Puerta, M. C.; Valerga, P. *J. Chem. Soc., Dalton Trans.* **1996**, 377.
(26) Jiménez-Tenorio, M.; Puerta, M. C.; Valerga, P. *J. Organomet. Chem.* **2000**, *609*, 161.

[Cp*Ru(PEt$_3$)$_2$][BAr′$_4$] (1). To a solution of [Cp*RuCl(PEt$_3$)$_2$] (0.25 g, 0.5 mmol) in fluorobenzene (15 mL) was added solid NaBAr′$_4$ (0.44 g, 0.5 mmol). The mixture was stirred for 15 min at room temperature. The initial orange solution was rapidly converted to a deep blue suspension. Sodium chloride was removed by filtration through Celite. The resulting solution was layered with petroleum ether and left standing undisturbed at room temperature. Well-formed blue crystals were obtained by slow diffusion of the petroleum ether into the fluorobenzene solution. These crystals were isolated by cannulating off the supernatant liquor and dried under an argon stream. Yield: 0.38 g, 57%. Anal. Calcd for $C_{54}H_{57}BF_{24}P_2Ru$: C, 48.5; H, 4.27. Found: C, 48.2; H, 4.12. Spectral data for **1** are as follows. ^{1}H NMR (400 MHz, CD_2Cl_2, 213 K): δ 1.11 (br, P(CH$_2$C*H*$_3$)$_3$), 1.30 (s, C$_5$(C*H*$_3$)$_5$), 1.91 (m, P(C*H*$_2$CH$_3$)$_3$). ^{31}P{^{1}H} NMR (161.89 MHz, CD_2Cl_2, 213 K): δ 20.4. The exceeding instability of this complex in solution prevented the recording of its ^{13}C{^{1}H} NMR spectrum.

[Cp*Ru(dippe)][BAr′$_4$] (2). This compound was obtained in a fashion analogous to that for **1**, starting from [Cp*RuCl(dippe)] (0.27 g, 0.5 mmol) and NaBAr′$_4$ (0.44 g, 0.5 mmol) in fluorobenzene (15 mL). Yield: 0.46 g, 68%. Anal. Calcd for $C_{56}H_{59}BF_{24}P_2Ru$: C, 49.4; H, 4.34. Found: C, 49.3; H, 4.40. Spectral data for **2** are as follows. ^{1}H NMR (400 MHz, CD_2Cl_2, 193 K): δ −4.94 (1 H, br, Ru−*H*−CH$_2$), 0.60, 0.84 (m br, P(CH(C*H*$_3$)$_2$)$_2$), 1.43 (s, C$_5$(C*H*$_3$)$_5$), 1.60 (d, PC*H*$_2$), 2.43 (m br, P(C*H*(CH$_3$)$_2$)$_2$). ^{31}P{^{1}H} NMR (161.89 MHz, CD_2Cl_2, 193 K): δ 81.3. ^{13}C{^{1}H} NMR (100.58 MHz, CD_2Cl_2, 193 K): δ 10.8 (s, C$_5$(*C*H$_3$)$_5$), 16.6, 17.2 (s, P(CH(*C*H$_3$)$_2$)$_2$), 18.1 (m, P*C*H$_2$), 26.2 (m, P(*C*H(CH$_3$)$_2$)$_2$), 83.2 (s, *C*$_5$(CH$_3$)$_5$).

[Cp*Ru(PMe^{i}Pr$_2$)$_2$][BAr′$_4$] (3). A solution of [Cp*RuCl(PMe^{i}Pr$_2$)] (0.2 g, 0.5 mmol) in fluorobenzene (15 mL) was treated with a slight excess over the stoichiometric amount of PMe^{i}Pr$_2$ (0.1 mL). When the mixture was stirred for a few minutes at room temperature, NaBAr′$_4$ (0.44 g, 0.5 mmol) was added. A color change to deep blue was observed. The mixture was stirred for 15 min. Sodium chloride was removed by filtration through Celite. The filtrate was layered with petroleum ether and left undisturbed at room temperature. Blue crystals were obtained by slow diffusion of petroleum ether into the fluorobenzene, were separated from the supernatant liquor, and were dried under an argon stream. Yield: 0.45 g, 66%. Anal. Calcd for $C_{56}H_{61}BF_{24}P_2Ru$: C, 49.3; H, 4.48. Found: C, 49.5; H, 4.42. Spectral data for **3** are as follows. ^{1}H NMR (400 MHz, CD_2Cl_2, 198 K): δ 0.67, 1.10 (m br, P(CH(C*H*$_3$)$_2$)$_2$), 1.34 (s, C$_5$(C*H*$_3$)$_5$), 1.48 (m, PC*H*$_3$), 2.13 (m br, P(C*H*(CH$_3$)$_2$)$_2$). ^{31}P{^{1}H} NMR (161.89 MHz, CD_2Cl_2, 198 K): δ 26.7. ^{13}C{^{1}H} NMR (100.58 MHz, CD_2Cl_2, 198 K): δ 3.27 (m, P*C*H$_3$), 11.0 (s, C$_5$(*C*H$_3$)$_5$), 17.6, 19.1 (s, P(CH(*C*H$_3$)$_2$)$_2$), 26.9 (d, J(C,P) = 22 Hz, P(*C*H(CH$_3$)$_2$)$_2$), 79.9 (s, *C*$_5$(CH$_3$)$_5$).

[Cp*Ru(η^6-C$_6$H$_5$F)][BAr′$_4$] (4). Compound **4** was often formed either as the final product or as a byproduct of the reaction of Cp*Ru phosphine halo complexes with NaBAr′$_4$ in fluorobenzene. It can be efficiently prepared by addition of NaBAr′$_4$ (0.89 g, 1 mmol) to [{Cp*RuCl}$_4$] (0.27 g, 0.25 mmol) in fluorobenzene (15 mL). The mixture was stirred at room temperature for 15 min. Then, it was filtered through Celite, layered with petroleum ether, and allowed to stand at room temperature. Large colorless crystals were obtained by slow diffusion of petroleum ether into the fluorobenzene solution. The crystals were separated from the mother liquor, washed with petroleum ether, and dried in vacuo. Yield: 0.76 g, 63%. Anal. Calcd for $C_{48}H_{32}BF_{25}Ru$: C, 48.2; H, 2.68. Found: C, 47.9; H, 2.55. Spectral data for **4** are as follows. ^{1}H NMR (400 MHz, CD_2Cl_2): δ 1.43 (s, C$_5$(C*H*$_3$)$_5$), 6.03, 6.21, 6.47(m, C$_6$*H*$_5$F). ^{13}C{^{1}H} NMR (100.58 MHz, CD_2Cl_2): δ 10.5 (s, C$_5$(*C*H$_3$)$_5$); 79.5, 87.6, 87.5 (*C*$_6$H$_5$F); 98.61 (s, *C*$_5$(CH$_3$)$_5$).

[Cp*Ru(PPh$_3$)$_2$][BAr′$_4$] (5). This compound was obtained in the form of a sticky blue solid, following a procedure analogous to that for **1**, starting from [Cp*RuCl(PPh$_3$)$_2$] (0.79 g, 0.5 mmol) and NaBAr′$_4$ (0.44 g, 0.5 mmol) in fluorobenzene. Yield: 0.66 g, 55%. Complex **5** is unstable and gradually turns into a yellow oily material, which consists of a mixture of the sandwich derivatives [Cp*Ru(η^6-C$_6$H$_5$PPh$_2$)][BAr′$_4$] (**5a**) and [Cp*Ru(η^6-C$_6$H$_5$POPh$_2$)][BAr′$_4$] (**5b**). For this reason, it was not analyzed. Spectral data for **5** are as follows. ^{1}H NMR (400 MHz, CD_2Cl_2): δ 1.11 (s, C$_5$(C*H*$_3$)$_5$), 7.05, 7.35, 7.41 (m br, P(C$_6$*H*$_5$)$_3$). ^{31}P{^{1}H} NMR (161.89 MHz, CD_2Cl_2): δ 33.8. ^{13}C{^{1}H} NMR (100.58 MHz, CD_2Cl_2): δ 10.1 (s, C$_5$(CH$_3$)$_5$), 82.3 (s, *C*$_5$(CH$_3$)$_5$), 128.7, 130.9, 133.5 (P(*C*$_6$H$_5$)$_3$). Selected spectral data for [Cp*Ru(η^6 -C$_6$H$_5$PPh$_2$)][BAr′$_4$] (**5a**) are as follows. ^{1}H NMR (400 MHz, CD_2Cl_2): δ 1.99 (s, C$_5$(C*H*$_3$)$_5$), 5.42, 5.52, 5.66 (m br, η^6-PC$_6$*H*$_5$), 7.1−7.7 (m, PC$_6$*H*$_5$). ^{31}P{^{1}H} NMR (161.89 MHz, CD_2Cl_2): δ −13.6. Selected spectral data for [Cp*Ru(η^6-C$_6$H$_5$POPh$_2$)][BAr′$_4$] (**5b**) are as follows. ^{1}H NMR (400 MHz, CD_2Cl_2): δ 1.99 (s, C$_5$(C*H*$_3$)$_5$), 5.77, 5.98 (η^6-POC$_6$*H*$_5$), 7.2−7.7 (POC$_6$*H*$_5$). ^{31}P{^{1}H} NMR (161.89 MHz, CD_2Cl_2): δ 31.3.

[Cp*Ru(PPh^{i}Pr$_2$)$_2$][BAr′$_4$] (6). This compound was obtained in a fashion analogous to that for **3**, starting from [Cp*RuCl(PPh^{i}Pr$_2$)] (0.15 g, 0.33 mmol), PPh^{i}Pr$_2$ (0.1 mL, excess), and NaBAr′$_4$ (0.3 g, 0.33 mmol) in fluorobenzene. Yield: 0.34 g, 69%. As is the case for compound **5**, complex **6** is also unstable, and it was not analyzed. It gradually turns into a yellow-brown oily material, which consists of a mixture of the sandwich derivatives [Cp*Ru(η^6-C$_6$H$_5$P^{i}Pr$_2$)][BAr′$_4$] (**6a**) and [Cp*Ru(η^6-C$_6$H$_5$PO^{i}Pr$_2$)][BAr′$_4$] (**6b**). Spectral data for **6** are as follows. ^{1}H NMR (400 MHz, CD_2Cl_2, 198 K): δ 1.06 (s, C$_5$(C*H*$_3$)$_5$), 1.25 (m br, P(CH(C*H*$_3$)$_2$)$_2$), 2.63 (m br, P(C*H*(CH$_3$)$_2$)$_2$), 6.93, 7.26, 7.43 (m, P(C$_6$*H*$_5$)). ^{31}P{^{1}H} NMR (161.89 MHz, CD_2Cl_2): δ 39.6. ^{13}C{^{1}H} NMR (100.58 MHz, CD_2Cl_2): δ 11.1 (s, C$_5$(*C*H$_3$)$_5$), 18.9, 20.0 (s, P(CH(*C*H$_3$)$_2$)$_2$), 28,1 (m, P(*C*H(CH$_3$)$_2$)$_2$), 79.7 (s, *C*$_5$(CH$_3$)$_5$), 128.2, 131.9, 135.0 (P(*C*$_6$H$_5$)). Selected spectral data for [Cp*Ru(η^6-C$_6$H$_5$P^{i}Pr$_2$)][BAr′$_4$] (**6a**) are as follows. ^{1}H NMR (400 MHz, CD_2Cl_2): δ 1.98 (s, C$_5$(C*H*$_3$)$_5$), 1.18, 1.21 (m, P(CH(C*H*$_3$)$_2$)$_2$), 2.19 (m, P(C*H*(CH$_3$)$_2$)$_2$), 5.35, 5.66 (m, η^6 - PC$_6$*H*$_5$). ^{31}P{^{1}H} NMR (161.89 MHz, CD_2Cl_2): δ 12.1. Selected spectral data for [Cp*Ru(η^6-C$_6$H$_5$PO^{i}Pr$_2$)][BAr′$_4$] (**6b**): δ 1.98 (s, C$_5$(C*H*$_3$)$_5$), 1.04, 1.09, 1.25 (m, PO(CH(C*H*$_3$)$_2$)$_2$), 2.12, 2.40 (m, PO(C*H*(CH$_3$)$_2$)$_2$), 5.72 (m, η^6-POC$_6$*H*$_5$). ^{31}P{^{1}H} NMR (161.89 MHz, CD_2Cl_2): δ 52.8.

[Cp*Ru(PR$_3$)$_3$][BAr′$_4$] (R = Et (7), Me (8)). To a solution of [Cp*RuCl(PR$_3$)$_2$] (0.2 mmol) in fluorobenzene were added PR$_3$ (R = Et for **7** and R -= Me for **8**; 0.05 mL, excess) and NaBAr′$_4$ (0.18 g, ca. 0.2 mmol). The resulting yellow solution was stirred for 10 min at room temperature, filtered through Celite, and layered with petroleum ether. The resulting well-formed yellow crystals were separated from the mother liquor, washed with petroleum ether, and dried in vacuo. Data for **7** are as follows. Yield: 0.25 g, 87%. Anal. Calcd for $C_{60}H_{72}BF_{24}P_3Ru$: C, 49.6; H, 4.96. Found: C, 49.4; H, 5.03. Spectral data for **7** are as follows. ^{1}H NMR (400 MHz, CD_3COCD_3): δ 1.23 (m, PCH$_2$C*H*$_3$), 1.74 (s, C$_5$(C*H*$_3$)$_5$), 2.01 (m, PC*H*$_2$CH$_3$). ^{31}P-{^{1}H} NMR (161.89 MHz, CD_3COCD_3): δ 21.33. ^{13}C{^{1}H} NMR (100.58 MHz, CD_3COCD_3): δ 11.30 (m, PCH$_2$*C*H$_3$), 11.48 (C$_5$-(*C*H$_3$)$_5$), 25.24 (m, P*C*H$_2$CH$_3$), 95.33 (*C*$_5$(CH$_3$)$_5$). Data for **8** are as follows. Yield: 0.24 g, 88%. Anal. Calcd for $C_{51}H_{54}BF_{24}P_3Ru$: C, 46.1; H, 4.07. Found: C, 45.8; H, 3.99. Spectral data for **8** are as follows. ^{1}H NMR (400 MHz, $CDCl_3$): δ 1.37 (m, PC*H*$_3$), 1.70 (s, C$_5$(C*H*$_3$)$_5$). ^{31}P{^{1}H} NMR (161.89 MHz, $CDCl_3$): δ 2.26. ^{13}C{^{1}H} NMR (100.58 MHz, $CDCl_3$): δ 11.50 (C$_5$(*C*H$_3$)$_5$), 22.68 (m, P*C*H$_3$), 95.82 (*C*$_5$(CH$_3$)$_5$).

The complexes **7** and **8** can be also isolated as BPh$_4^-$ salts, by treatment of [Cp*RuCl(PR$_3$)$_2$] with 1 equiv of either PEt$_3$ or PMe$_3$ and an excess of NaBPh$_4$ in MeOH. The resulting yellow precipitate is filtered, washed with EtOH and petroleum ether, and dried in vacuo. The complexes can be recrystallized from acetone/EtOH.

[Cp*RuH$_2$(PPh^{i}Pr$_2$)$_2$][BAr′$_4$] (9). To [{Cp*RuCl}$_4$] (0.12 g, 0.11 mmol) in fluorobenzene (10 mL) was added PPh^{i}Pr$_2$ (0.2 mL, 0.9 mmol). To this purple solution, under a hydrogen atmosphere, was added NaBAr′$_4$ (0.39 g, 0.44 mmol). The reaction mixture slowly becomes pale. It was stirred for 30

min and filtered through Celite. Evaporation of solvent to dryness gave a white crystalline solid. It was washed with petroleum ether and dried. Yield: 0.13 g, 80%. Anal. Calcd for $C_{66}H_{67}BF_{24}P_2Ru$: C, 53.2; H, 4.50. Found: C, 53.2; H, 4.46. Spectral data for **9** are as follows. ^{1}H NMR (400 MHz, CD_3COCD_3): δ −8.77 (t, ^2J(H,P) = 28.4 Hz, RuH_2), 1.56 (s, $C_5(CH_3)_5$), 1.25 (m, P(CH(CH_3)$_2$)$_2$), 2.38 (m, P(CH(CH$_3$)$_2$)$_2$), 7.52, 7.54, 7.59 (m, PC_6H_5). ^{1}H NMR (400 MHz, CD_2Cl_2, 193 K): major isomer, δ −9.43 (t, $^2J(H_A,P)$ = 33.9 Hz, RuH_AH_B), −9.19 (t, $^2J(H_B,P)$ = 23.8 Hz, RuH$_A$$H_B$); minor isomer, δ −9.03 (t, ^2J(H,P) = 30.2 Hz, RuH_2). ^{31}P{^{1}H} NMR (161.89 MHz, CD_3COCD_3): δ 70.27. ^{31}P{^{1}H} NMR (161.89 MHz, CD_2Cl_2, 193 K): major isomer (83% at 193 K), δ 64.3 (d, $J(P_A,P_B)$ = 22 Hz, P_A), 70.9 (d, $J(P_A,P_B)$ = 22 Hz, P_B); minor isomer (17% at 193 K), δ 62.4 (d, $J(P_A,P_B)$ = 19.5 Hz, P_A), 71.9 (d, $J(P_A,P_B)$ = 19.5, P_B). ^{13}C{^{1}H} NMR (100.58 MHz, $CDCl_3$): δ 10.35 (s, $C_5(CH_3)_5$), 18.92, 20.32 (s, P(CH(CH_3)$_2$)$_2$), 27.47 (m, P(CH(CH$_3$)$_2$)$_2$), 100.72 (s, $C_5(CH_3)_5$), 128.30, 130.65, 132.32 (PC_6H_5).

[Cp*RuH(PPh^{i}Pr$_2$)$_2$] (10). A THF solution of [Cp*RuH_2(PPh^{i}Pr$_2$)$_2$][BAr′$_4$] was treated with an excess of solid KO^{t}Bu. The reaction mixture was stirred at room temperature for 1 h. Then the solvent was removed in vacuo. The residue was extracted with petroleum ether, and the extracts were filtered through Celite. Concentration and cooling to −20 °C gave a pale yellow residue. Yield: 60−70%. Anal. Calcd for $C_{34}H_{54}P_2Ru$: C, 65.3; H, 8.64. Found: C, 64.9; H, 8.40. Spectral data for **10** are as follows. ^{1}H NMR (400 MHz, C_6D_6): δ −13.78 (t, ^2J(H,P) = 36 Hz), 1.48 (s, $C_5(CH_3)_5$), 1.26, 1.11, 0.96 (m, P(CH(CH_3)$_2$)$_2$), 2.04 (m, br, P(CH(CH$_3$)$_2$)$_2$), 7.58, 7.60, 7.69 (m, PC_6H_5). ^{31}P{^{1}H} NMR (161.89 MHz, C_6D_6): δ 77.03. ^{13}C{^{1}H} NMR (100.58 MHz, C_6D_6): δ 12.05 (s, $C_5(CH_3)_5$), 19.64, 20.69, 21.20, 22.58 (s, P(CH(CH_3)$_2$)$_2$), 27.70, 29.27 (m, P(CH(CH$_3$)$_2$)$_2$), 90.64 (s, $C_5(CH_3)_5$), 126.54, 131.09, 131.96, 133.92 (PC_6H_5).

[Cp*RuH$_2$(PPh$_3$)$_2$][BAr′$_4$] (11). To [Cp*RuCl(PPh$_3$)$_2$] (0.12 g, 0.15 mmol) in fluorobenzene (10 mL) was added NaBAr′$_4$ (0.133 g, 0.15 mmol) under a hydrogen atmosphere. The reaction mixture slowly became pale. It was stirred for 30 min and filtered through Celite. Evaporation of solvent to dryness gave a pale yellow glassy solid which crystallized on cooling. It was washed with petroleum ether and dried. Yield: 0.17 g, 70%. Anal. Calcd for $C_{78}H_{59}BF_{24}P_2Ru$: C, 57.6; H, 3.63. Found: C, 57.7; H, 3.56. Selected spectral data for **11** are as follows. ^{1}H NMR (400 MHz, CD_2Cl_2): δ −7.28 (t, ^2J(H,P) = 26.4 Hz), 1.36 (s, $C_5(CH_3)_5$), 7.30, 7.35, 7.48 (m, PC_6H_5). ^{31}P{^{1}H} NMR (161.89 MHz, CD_2Cl_2): δ 63.20. ^{13}C{^{1}H} NMR (100.58 MHz, CD_2Cl_2): δ 9.94 ($C_5(CH_3)_5$), 101.67 ($C_5(CH_3)_5$), 128.72, 131.03, 133.99, 135.19 (PC_6H_5).

[Cp*RuHCl(PEt$_3$)$_2$][BAr′$_4$] (12). To a solution of [Cp*RuCl(PEt$_3$)$_2$] (0.1 g, ca. 0.2 mmol) in 5 mL of fluorobenzene were added a 5 mL ether solution containing anhydrous HCl (ca. 0.4 mmol, generated by reaction of 25 μL of SiCl(CH$_3$)$_3$ with 6 μL of MeOH) and NaBAr′$_4$ (0.17 g, 0.196 mmol). The reaction mixture is yellow. It was stirred for 30 min and filtered through Celite. Evaporation of solvent gave a yellow-orange solid. It was washed with petroleum ether and dried. Yield: 0.19 g, 70%. Anal. Calcd for $C_{54}H_{58}BClF_{24}P_2Ru$: C, 47.3; H, 4.23. Found: C, 47.0; H, 4.15. Spectral data for **12** are as follows. ^{1}H NMR (400 MHz, CD_3COCD_3): δ −9.68 (t, ^2J(H,P) = 31.2 Hz), 1.24 (m, PCH$_2$CH_3), 1.89 (s, $C_5(CH_3)_5$), 2.16, 2.00 (m, PCH_2CH$_3$). ^{31}P{^{1}H} NMR (161.89 MHz, CD_3COCD_3): δ 33.31. ^{13}C{^{1}H} NMR (100.58 MHz, CD_3COCD_3): δ 9.27 (PCH$_2$CH_3), 10.21 (s, $C_5(CH_3)_5$), 20.11, 20.42 (m, PCH_2CH$_3$), 104.21 (s, $C_5(CH_3)_5$).

[Cp*RuHCl(dippe)][BAr′$_4$] (13). This compound was obtained in a fashion analogous to that for **12**, starting from [Cp*RuCl(dippe)]. Alternatively, it can be prepared by direct reaction of **2** with anhydrous HCl in diethyl ether. Yield: quantitative. Anal. Calcd for $C_{56}H_{60}BClF_{24}P_2Ru$: C, 48.1; H, 4.29. Found: C, 48.2; H, 4.08. Spectral data for **13** are as follows. ^{1}H NMR (400 MHz, CD_3COCD_3): δ −9.95 (t, ^2J(H,P) = 30.3 Hz), 1.97 (s, $C_5(CH_3)_5$), 2.09 (m, PCH_2), 2.45, 3.11 (m, P(CH(CH$_3$)$_2$)$_2$). ^{31}P{^{1}H} NMR (161.89 MHz, CD_3COCD_3): δ 71.64. ^{13}C{^{1}H} NMR (100.58 MHz, CD_3COCD_3): δ 10.89 (s, $C_5(CH_3)_5$), 19.06, 19.21, 19.30, 21.09 (s, P(CH(CH_3)$_2$)$_2$), 21.17 (m, PCH_2), 26.35 (m, P(CH(CH$_3$)$_2$)$_2$), 104.02 (s, $C_5(CH_3)_5$).

[Cp*RuHCl(PMe^{i}Pr$_2$)$_2$][BAr′$_4$] (14). To a solution of **3** (0.14 g, ca. 0.1 mmol) in 5 mL of dichloromethane was added 1 drop of concentrated hydrochloric acid. The color changed immediately to yellow-orange. Concentration and addition of petroleum ether gave a yellow-orange solid, which was washed with petroleum ether and dried. Yield: 0.14 g, quantitative. Anal. Calcd for $C_{56}H_{62}BClF_{24}P_2Ru$: C, 48.0; H, 4.43. Found: C, 47.8; H, 4.36. Spectral data for **14** are as follows. ^{1}H NMR (400 MHz, CD_3COCD_3): δ −9.24 (t, ^2J(H,P) = 30.3 Hz), 1.28 (m, P(CH(CH_3)$_2$)$_2$), 1.42 (d, PCH_3),1.89 (s, $C_5(CH_3)_5$), 2.30 (m, P(CH(CH$_3$)$_2$)$_2$). ^{31}P{^{1}H} NMR (161.89 MHz, CD_3COCD_3): δ 39.17. ^{13}C{^{1}H} NMR (100.58 MHz, CD_3COCD_3): δ 6.78 (d, J(C,P) = 27.4 Hz, PCH_3), 10.72 (s, $C_5(CH_3)_5$), 19.08, 19.35, 20.03, 20.51 (s, P(CH(CH_3)$_2$)$_2$), 29.24 (t, J(C,P) = 29.6 Hz, P(CH(CH$_3$)$_2$)$_2$), 104.02 (s, $C_5(CH_3)_5$).

X-ray Structure Determinations. Crystals of **1**−**4**, **7**, and **9** were obtained by slow diffusion of petroleum ether into fluorobenzene solutions. Crystal data and experimental details are given in Table 1. X-ray data were collected on a Bruker AXS Smart CCD area detector diffractometer (graphite-monochromated Mo Kα radiation, λ = 0.710 73 Å, 0.3° ω-scan frames covering complete spheres of the reciprocal space). Corrections for Lorentz and polarization effects, for crystal decay, and for absorption were applied. All structures were solved by direct methods using the program SHELXS97.[27a] Structure refinement on F^2 was carried out with the program SHELXL97[27b] for **1**−**3**, **7**, and **9** and SHELXH97[27c] for **4**. All non-hydrogen atoms were refined anisotropically. Hydrogen atoms were inserted in idealized positions and were refined riding with the atoms to which they were bonded.

Computational Details. All calculations were performed using the Gaussian98[28] software package on the Silicon Graphics Power Challenge of the Vienna University of Technology. To reduce computational effort, [Cp*Ru(PEt$_3$)$_2$]$^+$, [Cp*Ru(dippe)]$^+$, or [Cp*Ru(PMe^{i}Pr$_2$)$_2$]$^+$ and related diamine complexes such as [Cp*Ru(Me$_2$NCH$_2$CH$_2$NR$_2$)]$^+$ (R = Me, ^{i}Bu) were modeled by the smaller entities [CpRu(PH$_3$)$_2$]$^+$, [CpRu(H$_2$PCH$_2$CH$_2$PH$_2$)]$^+$, [CpRu(H$_2$NCH$_2$CH$_2$NH$_2$)]$^+$, and [CpRu(NH$_3$)$_2$]$^+$. The geometry and energy of the 16e complexes as well as the 18e complexes *trans*-[CpRu(H$_2$PCH$_2$CH$_2$PH$_2$)(H)$_2$]$^+$, [CpRu(H$_2$PCH$_2$CH$_2$PH$_2$)(η^2-H$_2$)]$^+$, *trans*-[CpRu(PH$_3$)$_2$(H)$_2$]$^+$, and [CpRu(PH$_3$)$_2$(η^2-H$_2$)]$^+$ were optimized at the B3LYP level[29] with the Stuttgart/Dresden ECP (SDD) basis set[30] to describe the electrons of the ruthenium atom. For all other atoms the

(27) (a) SHELXS97, Program for Crystal Structure Solution; University of Göttingen, Göttingen, Germany, 1990. (b) SHELXL97, Program for Crystal Structure Refinement; University of Göttingen, Göttingen, Germany, 1997. (c) SHELXH97, Special Version of SHELXL97 for the Refinement of Very Large Structures; University of Göttingen, Göttingen, Germany, 1997.

(28) Frisch, M. J.; Trucks, G. W.; Schlegel, H. B.; Scuseria, G. E.; Robb, M. A.; Cheeseman, J. R.; Zakrzewski, V. G.; Montgomery, J. A., Jr.; Stratmann, R. E.; Burant, J. C.; Dapprich, S.; Millam, J. M.; Daniels, A. D.; Kudin, K. N.; Strain, M. C.; Farkas, O.; Tomasi, J.; Barone, V.; Cossi, M.; Cammi, R.; Mennucci, B.; Pomelli, C.; Adamo, C.; Clifford, S.; Ochterski, J.; Petersson, G. A.; Ayala, P. Y.; Cui, Q.; Morokuma, K.; Malick, D. K.; Rabuck, A. D.; Raghavachari, K.; Foresman, J. B.; Cioslowski, J.; Ortiz, J. V.; Stefanov, B. B.; Liu, G.; Liashenko, A.; Piskorz, P.; Komaromi, I.; Gomperts, R.; Martin, R. L.; Fox, D. J.; Keith, T.; Al-Laham, M. A.; Peng, C. Y.; Nanayakkara, A.; Gonzalez, C.; Challacombe, M.; Gill, P. M. W.; Johnson, B. G.; Chen, W.; Wong, M. W.; Andres, J. L.; Head-Gordon, M.; Replogle, E. S.; Pople, J. A. *Gaussian 98*, revision A.5; Gaussian, Inc.: Pittsburgh, PA, 1998.

(29) Becke, A. D. *J. Chem. Phys.* **1993**, *98*, 5648. Miehlich, B.; Savin, A.; Stoll, H.; Preuss, H. *Chem. Phys. Lett.* **1989**, *157*, 200. Lee, C.; Yang, W.; Parr, G. *Phys. Rev. B* **1988**, *37*, 785.

(30) (a) Haeusermann, U.; Dolg, M.; Stoll, H.; Preuss, H. *Mol. Phys.* **1993**, *78*, 1211. (b) Kuechle, W.; Dolg, M.; Stoll, H.; Preuss, H. *J. Chem. Phys.* **1994**, *100*, 7535. (c) Leininger, T.; Nicklass, A.; Stoll, H.; Dolg, M.; Schwerdtfeger, P. *J. Chem. Phys.* **1996**, *105*, 1052.

Table 1. Summary of Crystallographic Files for Compounds 2−4, 7, and 9

	2	3	4	7	9
formula	$C_{56}H_{59}BF_{24}P_2Ru$	$C_{56}H_{61}BF_{24}P_2Ru$	$C_{48}H_{32}BF_{25}Ru$	$C_{60}H_{72}BF_{24}P_3Ru$	$C_{66}H_{67}BF_{24}P_2Ru$
fw	1361.85	1363.87	1195.62	1453.97	1490.02
T (K)	213(2)	223(2)	223(2)	223(2)	173(2)
cryst size (mm)	0.70 × 0.70 × 0.70	0.80 × 0.70 × 0.70	0.80 × 0.40 × 0.30	0.70 × 0.65 × 0.60	0.72 × 0.40 × 0.40
cryst syst	triclinic	monoclinic	monoclinic	monoclinic	monoclinic
space group	$P\bar{1}$ (No. 2)	$P2_1$ (No. 4)	$P2_1/c$ (No. 14)	$P2_1/c$ (No. 14)	$P2_1/n$ (No. 14)
cell params					
a (Å)	12.597(6)	12.474(5)	12.830(12)	19.447(5)	12.284(3)
b (Å)	12.946(6)	18.974(8)	58.17(6)	13.750(4)	15.105(4)
c (Å)	18.967(9)	13.003(5)	20.348(19)	26.068(6)	36.404(9)
α (deg)	95.40(2)				
β (deg)	99.62(2)	92.68(2)	104.71(2)	107.42(2)	99.14(1)
γ (deg)	92.78(2)				
V (Å^3)	3030(2)	3074(2)	14688(25)	6651(3)	6669(3)
Z	**2**	**2**	**12**	**4**	**4**
ρ_{calcd} (g cm^{-3})	1.493	1.473	1.622	1.452	1.484
λ(Mo Kα) (Å)	0.71073	0.71073	0.71073	0.71073	0.71073
μ(Mo Kα) (cm^{-1})	4.21	4.15	4.50	4.12	3.90
F(000)	1380	1384	7128	2968	3032
max and min transmissn factors	0.80−0.72	0.83−0.76	1.00−0.87	1.00−0.88	1.00−0.92
θ range for data collection (deg)	1.8−30.0	1.9−30.0	2.0−24.0	1.7−30.0	2.2−30.0
no. of rflns collected	44 116	67 375	135 060	69 930	93 030
no. of unique rflns (R_{int})	17 192 (0.021)	17 644 (0.021)	22 779 (0.038)	19 015 (0.031)	19 071 (0.027)
no. of obsd reflections ($I > 2\sigma_I$)	14 100	15 719	19 241	13 862	15 788
no. of params	816	758	2055	874	926
final R1, wR2 values ($I > 2\sigma_I$)	0.0538, 0.1433	0.0605, 0.1684	0.0643, 0.1433	0.0443, 0.1071	0.0445, 0.1029
final R1, wR2 values (all data)	0.0665, 0.1566	0.0679, 0.1789	0.0756, 0.1496	0.0677, 0.1252	0.0573, 0.1105
goodness of fit on F^2	1.027	1.022	1.049	1.023	1.056
residual electron density peaks (e Å^{-3})	+1.03/−0.70	+1.36/−1.04	+0.961/−0.53	+0.58/−0.62	+0.67/−0.60

6-31G** basis set was employed.[31] Frequency calculations were performed to confirm the nature of the stationary points, yielding no imaginary frequency for the minima. All geometries were optimized without constraints (C_1 symmetry), and the energies were zero point corrected.

Results and Discussion

Synthesis and Structure of 16e Complexes. The complexes [Cp*RuCl(PEt_3)$_2$] and [Cp*RuCl(dippe)] react with NaBAr′$_4$ in fluorobenzene under argon to give the cationic 16e complexes [Cp*Ru(PEt_3)$_2$][BAr′$_4$] (**1**) and [Cp*Ru(dippe)][BAr′$_4$] (**2**). In an analogous fashion, coordinatively unsaturated [Cp*Ru(PMe^iPr_2)$_2$][BAr′$_4$] (**3**) was obtained by treatment of [Cp*RuCl(PMe^iPr_2)] with PMe^iPr_2 (1 equiv) and NaBAr′$_4$ in fluorobenzene under argon. Attempts to obtain mixed-phosphine complexes such as [Cp*Ru(PMe^iPr_2)(PEt_3)][BAr′$_4$] proved so far to be unsuccessful. Compounds **1**−**3** are very air sensitive, diamagnetic, deep blue materials. The color arises from a strong band in the visible spectrum (CH_2Cl_2 solution) between 600 and 700 nm, characteristic of 16e half-sandwich ruthenium complexes.[9−18]

The X−ray crystal structures of **1**−**3** consist of closely related packings of complex cations and [BAr′$_4$]$^-$ anions separated by van der Waals contacts, without interaction with the metal centers. The [BAr′$_4$]$^-$ ions form in principle three-dimensional lattices with approximately quadratic channels (dimensions of the squarelike grids of about 12.5−13.2 Å with a mutual angle of 93−94°, translation period along the channel about 19 Å), which host the cations arranged in a zigzag-like fashion (cf. Figure S3 of the Supporting Information). The cations show two-legged piano-stool structures with significant differences in the orientation of the P-bonded alkyl groups relative to the Cp* moieties. In the case of **1**, the [BAr′$_4$]$^-$ anion and the Cp*Ru moiety are reasonably ordered, but the PEt_3 ligands were found to be heavily disordered around the ruthenium atom. Attempts to model the disorder were made by considering two complex cations with a relative occupancy factor of 0.5 each and different positions of the phosphorus atoms and ethyl groups of the PEt_3 ligands. Unfortunately, the structural disorder prohibited the determination of accurate bond lengths and angles. All relevant X-ray data, including figures, have been deposited as Supporting Information for reference. In sum, the raw molecular skeleton obtained from diffraction experiments points in the case of **1** to a genuine 16-electron species possibly stabilized by an agostic interaction. An important structural parameter is the degree of pyramidalization of the 16e complex, measurable by the angle of pyramidalization α, defined as the angle formed by the centroid of the Cp* ring, the ruthenium atom, and the centroid of the triangle defined by the atoms Ru, P(1), and P(2). For complex **1**, α is estimated to be ca. 170°. Solutions of **1** in fluorobenzene or dichloromethane are unstable, since the initially dark blue solutions gradually turn green and finally yellow. This suggests a steady conversion of the 16e cation into several more stable 18e species, namely [Cp*Ru(O_2)(PEt_3)$_2$]$^+$,[26] [Cp*Ru(N_2)(PEt_3)$_2$]$^+$,[26] and [Cp*Ru(PEt_3)$_3$]$^+$ (**5**; see Reactivity of the 16e Complexes). Therefore, crystallization of **1** was only achieved from concentrated solutions in a rather short period of time and the mother liquor was discarded, which usually becomes greenish. The instability in solution prevented clean NMR spectra

(31) (a) McClean, A. D.; Chandler, G. S. *J. Chem. Phys.* **1980**, *72*, 5639. (b) Krishnan, R.; Binkley, J. S.; Seeger, R.; Pople, J. A. *J. Chem. Phys.* **1980**, *72*, 650. (c) Wachters, A. H. *Chem. Phys.* **1970**, *52*, 1033. (d) Hay, P. J. *J. Chem. Phys.* **1977**, *66*, 4377. (e) Raghavachari, K.; Trucks, G. W. *J. Chem. Phys.* **1989**, *91*, 1062. (f) Binning, R. C.; Curtiss, L. A. *J. Comput. Chem.* **1995**, *103*, 6104. (g) McGrath, M. P.; Radom, L. *J. Chem. Phys.* **1991**, *94*, 511.

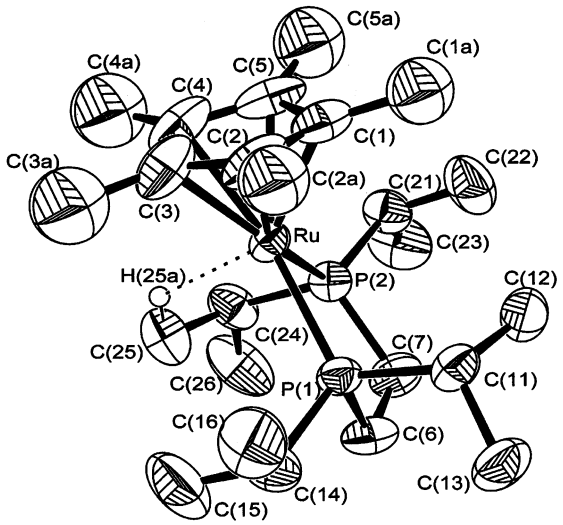

Figure 1. ORTEP drawing (50% thermal ellipsoids) of the cation $[Cp^*Ru(dippe)]^+$ in complex **2**. Hydrogen atoms, except H(25a) have been omitted. Selected bond lengths (Å) and angles (deg) with estimated standard deviations in parentheses: Ru−C(1), 2.179(3); Ru−C(2), 2.235(3); Ru−C(3), 2.211(3); Ru−C(4), 2.205(3); Ru−C(5), 2.203(3); Ru−P(1), 2.331(1); Ru−P(2), 2.356(1); Ru···C(25), 2.953(4); Ru···H(25a), 2.262 (calculated); P(1)−Ru−P(2), 83.13(4); Ru−P(2)−C(24), 99.46(12).

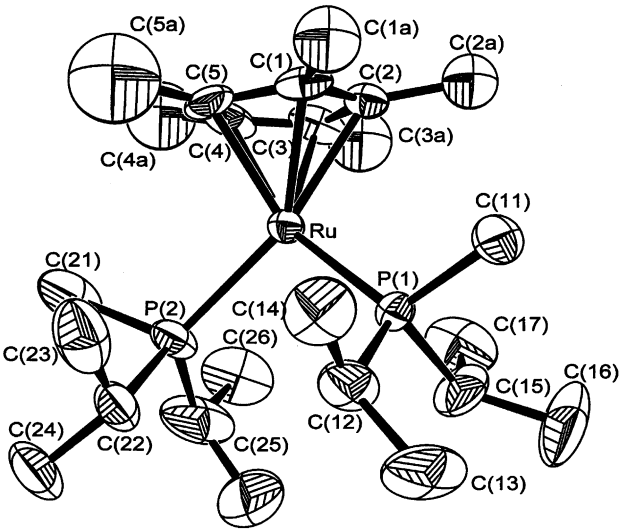

Figure 2. ORTEP drawing (50% thermal ellipsoids) of the cation $[Cp^*Ru(PMe^iPr_2)_2]^+$ in complex **3**. Hydrogen atoms have been omitted. Selected bond lengths (Å) and angles (deg) with estimated standard deviations in parentheses. Ru−C(1), 2.198(4); Ru−C(2), 2.205(5); Ru−C(3), 2.175(6); Ru−C(4), 2.206(5); Ru−C(5), 2.126(5); Ru−P(1), 2.395(1); Ru−P(2), 2.393(1); P(1)−Ru−P(2), 101.43(5).

(CD_2Cl_2) from being obtained. The resonances attributable to **1** were always deteriorated by signals stemming from follow-up products. Although the $^{31}P\{^1H\}$ NMR spectrum of **1** consists of one singlet, agostic interactions cannot be ruled out.

In fact, the ^1H NMR spectrum of **2** in CD_2Cl_2 at 193 K displays one broad resonance at −4.94 ppm, which clearly points to the presence of an agostic interaction in this particular case. The $^{31}P\{^1H\}$ NMR spectrum consists of one singlet at this temperature, and no decoalescence is observed. This suggests that there is rapid hydrogen scrambling with all of the isopropyl protons of the dippe ligand, rendering the phosphorus atoms equivalent in the NMR time scale. Also the X-ray structure of $[Cp^*Ru(dippe)]^+$ reveals an agostic interaction with a hydrogen atom of an isopropyl group (Figure 1). The observed Ru···C(25) separation is 2.953(4) Å (calculated Ru−H(25a) bond distance 2.262 Å). The Ru···C(25) distance is only slightly longer than the average Ru···C value of 2.875 Å observed for $[RuPh(CO)(PMe^tBu_2)_2][BAr'_4]$,[33] which contains two strong agostic interactions of the ^{t}Bu groups of the two phosphines. A shorter Ru···C distance of 2.651 Å (average) has been reported for $[RuCl_2\{PPh_2(C_6H_3Me_2)\}_2]$, showing two agostic Ru···H−C interactions of the methyl groups.[34] The Ru−P(2)−C(24) angle in **2** is 99.45°, in contrast to 117−124° in the case of nonagostic isopropyl groups. The $[Cp^*RuP_2]^+$ moiety adopts a bent (pyramidalized) conformation with $\alpha = 160°$.

No evidence of agostic interactions can be detected in the NMR spectra of **3**. Indeed, the spectra are very simple, just as expected for a compound of C_{2v} symmetry. The cation $[Cp^*Ru(PMe^iPr_2)_2]^+$ (Figure 2) displays a pseudo-C_{2v} structure, similar to that of $[Cp^*RuX(PR_3)]$, $[Cp^*Ru(TMEDA)][BAr'_4]$,[17,18] or [Cp*Ru(amidinate)].[16] Since the isopropyl groups are all directed away from the region perpendicular to the RuP_2 plane, agostic donation is absent. The shortest contact between Ru and the isopropyl carbon atoms is Ru···C(17) at 3.303(13) Å (shortest calculated R−H distance 2.67 Å to H(17a)), too far for agostic donation. The degree of pyramidalization for $[Cp^*Ru(PMe^iPr_2)_2]^+$ is minimal ($\alpha = 171°$).

Attempts to prepare $[Cp^*Ru(PR_3)_2][BAr'_4]$ ($PR_3 = P^iPr_3$, PCy_3) were unsuccessful. Halide abstraction from the corresponding neutral derivative $[Cp^*RuCl(PR_3)]$ in the presence of P^iPr_3 or PCy_3, using $Na[BAr'_4]$ in fluorobenzene as halide scavenger, did not yield any blue material, in contrast to **1**−**3**. Instead, large colorless chunky crystals were obtained, which contained no phosphorus, as inferred from the $^{31}P\{^1H\}$ NMR spectra. Furthermore, the isolated materials from both reactions turned out to be the same compound: viz., the 18e sandwich derivative $[Cp^*Ru(\eta^6\text{-}C_6H_5F)][BAr'_4]$ (**4**). Despite the poor coordinating abilities of halobenzenes,[35] the formation of π-complexes is a possibility to be considered when $Na[BAr'_4]$ in combination with fluorobenzene is used for the generation of highly reactive species. In fact, Cp*Ru π-complexes of highly fluorinated arenes are known, such as the series of derivatives $[Cp^*Ru(\eta^6\text{-}C_6F_{6-n}(OMe)_n)][CF_3SO_3]$ ($n = 0-2$).[36] In our particular case, halide abstraction from either $[Cp^*RuCl(P^iPr_3)]$ or $[Cp^*RuCl(PCy_3)]$ takes place with simultaneous phosphine loss and generation of the fragment $\{[Cp^*Ru]^+\}$, which is trapped by fluorobenzene, furnishing the sandwich complex **4**. The latter can alternatively be obtained in high yield by direct reaction of the tetramer $[\{Cp^*Ru(\mu\text{-}Cl)\}_4]$ with $Na[BAr'_4]$ in fluoroben-

(32) Johnson, C. K. ORTEP, A Thermal Ellipsoid Plotting Program; Oak Ridge National Laboratory, Oak Ridge, TN, 1965.

(33) (a) Huang, D.; Streib, W. E.; Eisenstein, O.; Caulton, K. G. *Angew. Chem., Int. Ed.* **1997**, *36*, 2005. (b) Huang, D.; Streib, W. E.; Bollinger, J. C.; Caulton, K. G.; Winter, R. F.; Scheiring, T. *J. Am. Chem. Soc.* **1999**, *121*, 8087.

(34) Baratta, W.; Herdtweck, E.; Rigo, P. *Angew. Chem., Int. Ed.* **1999**, *38*, 1629.

(35) Dembek, A. A.; Fagan, P. J. *Organometallics* **1995**, *14*, 3741.

(36) Koelle, U.; Hornig, A.; Englert, U. *Organometallics* **1994**, *13*, 4064.

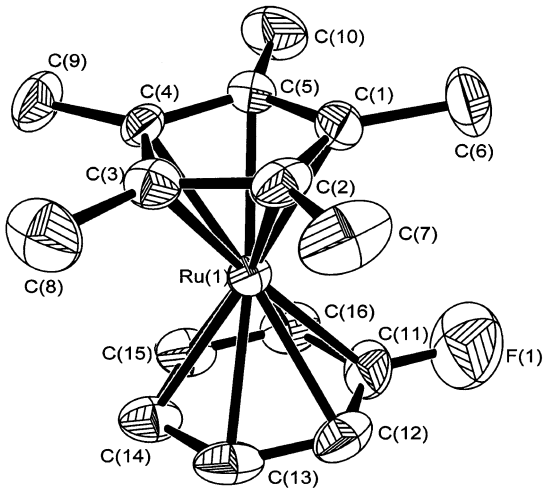

Figure 3. ORTEP drawing (50% thermal ellipsoids) of one of the three independent cations $[Cp^*Ru(\eta^6\text{-}C_6H_5F)]^+$ in complex **4**. Hydrogen atoms have been omitted. Selected bond lengths (Å) with estimated standard deviations in parentheses: Ru(1)−C(1), 2.171(5); Ru(1)−C(2), 2.181(5); Ru(1)−C(3), 2.167(6); Ru(1)−C(4), 2.178(5); Ru(1)−C(5), 2.179(5); Ru(1)−C(11), 2.174(6); Ru(1)−C(12), 2.198(6); Ru(1)−C(13), 2.217(6); Ru(1)−C(14), 2.241(6); Ru(1)−C(15), 2.210(6); Ru(1)−C(16), 2.207(6); C(11)−F(1), 1.301(9).

zene. This underlines the high affinity of the moiety $\{[Cp^*Ru]^+\}$ for aromatic systems.[35−38]

The reaction of $[Cp^*RuCl(PMe_3)_2]$ with $NaBAr'_4$ also failed to give the 16e compound $[Cp^*Ru(PMe_3)_2]^+$. Instead, a yellow-orange solution was obtained as a mixture of colorless crystals of the fluorobenzene sandwich complex **4** and yellow crystals of the tris(phosphine) derivative $[Cp^*Ru(PMe_3)_3][BAr'_4]$ (**6**). Hence, halide abstraction from $[Cp^*RuCl(PMe_3)_2]$ results in ligand redistribution:

$$[Cp^*RuCl(PMe_3)_2] \xrightarrow[FPh]{NaBAr'_4} \{[Cp^*Ru(PMe_3)_2]^+\} \longrightarrow \begin{cases} 2/3\ [Cp^*Ru(PMe_3)_3][BAr'_4] \\ + \\ 1/3\ [Cp^*Ru(FPh)][BAr'_4] \end{cases} \quad (1)$$

The crystal structure of **4** contains an asymmetric unit of three independent cation complexes and three $[BAr'_4]^-$ anions. One cationic complex is disordered in two possible orientations with fractional occupation factors of 0.69 and 0.31, respectively. The ORTEP[32] view in Figure 3 shows a sandwich structure with a planar π-complexed C_6H_5F ring. The dimension of coordinated fluorobenzene is similar to that found in other $\eta^6\text{-}C_6H_5F$ complexes.[39] Also, the closely related complex $[(\eta^5\text{-}C_5Me_4Et)Ru(\eta^6\text{-}C_6F_5OH)][CF_3SO_3]$ may be noted.[36] The ruthenium−fluorobenzene carbon bond distances in the latter compare well with the average value of 2.225 Å found in **4**. Furthermore, all Ru−C separations in **4** are in the range found for other RuCp(arene) cations.[21,37,38] It would appear that the stability of the 16e complexes of the type $[Cp^*Ru(PP)][BAr'_4]$ is critically dependent on the steric requirements of the phosphine ligands. If the phosphine is small (i.e. PMe_3), isolation is not feasible, since the metal center is not shielded against side reactions tending to attain the 18e configuration. On the other hand, overly bulky phosphines, such as P^iPr_3 and PCy_3, obviously do not form stable $[Cp^*Ru(PP)]^+$ cations. The increased steric pressure generated when two bulky phosphines are bound to a single Cp*Ru moiety may force longer metal−phosphorus separations. Consequently, the phosphine ligands are replaced by other donor molecules: i.e., arenes. This hypothesis is consistent with the sequence of relative $Ru-PR_3$ binding energies measured by Nolan and co-workers, confirming the lability of both P^iPr_3 and PCy_3 bound to the Cp*Ru moiety.[40]

Halide abstraction from $[Cp^*RuCl(PPh_3)_2]$ and $[Cp^*RuCl(PPh^iPr_2)]$ in the presence of PPh^iPr_2 using $NaBAr'_4$ in fluorobenzene gave, in both cases, deep blue solutions, from which blue solids could be isolated. However, the 16e complexes $[Cp^*Ru(PPh_3)_2][BAr'_4]$ (**5**) and $[Cp^*Ru(PPh^iPr_2)_2][BAr'_4]$ (**6**) could not be crystallized (in contrast to **1**−**3**) but decomposed to oily, yellow materials. The ^1H and $^{31}P\{^1H\}$ NMR spectra of freshly prepared solutions in CD_2Cl_2 are consistent with the 16e cations $[Cp^*Ru(PPh_3)_2]^+$ and $[Cp^*Ru(PPh^iPr_2)_2]^+$. No evidence for agostic interactions was found. On standing, signals corresponding to at least two different $\eta^6\text{-}C_6H_5$ groups appear in the ^1H NMR spectrum, whereas the $^{31}P\{^1H\}$ NMR spectrum displays new resonances arising at −13.6 and 31.3 ppm in the case of **5** and 12.1 and 52.8 ppm in the case of **6**. The high-field signals suggest the presence of PPh_3 and PPh^iPr_2 groups that were not coordinated through the phosphorus atom to the metal, whereas the resonances at lower fields suggest the presence of $POPh_3$ and $POPh^iPr_2$ groups, also not coordinated through phosphorus. We interpret these observations in terms of the rearrangement of the 16e into the 18e sandwich derivatives $[Cp^*Ru(\eta^6\text{-}C_6H_5PPh_2)]^+$ (**5a**) and $[Cp^*Ru(\eta^6\text{-}C_6H_5P^iPr_2)]^+$ (**6a**) plus free phosphine (Scheme 1). Trace amounts of oxygen caused metal-mediated phosphine oxidation, yielding the corresponding phosphine oxide. We and other authors have previously reported the formation of phosphine oxides in reactions of half-sandwich ruthenium complexes.[26,41−43] Furthermore, the system $[CpRuCl(PPh_3)_2]/NaClO_4$ acts as a catalyst for the oxidation of PPh_3 to $POPh_3$ in refluxing MeOH.[42] In addition, $POPh_3$ is known to coordinate to ruthenium in an η^6 fashion, as in $[CpRu(\eta^6\text{-}C_6H_5POPh_2)][ClO_4]$.[42] In the present case both $POPh_3$ and $POPh^iPr_2$ may behave in this way, furnishing $[Cp^*Ru(\eta^6\text{-}C_6H_5POPh_2)]^+$ (**5b**) and $[Cp^*Ru(\eta^6\text{-}C_6H_5PO^iPr_2)]^+$ (**6b**) (Scheme 1). These species may well be responsible for the additional set of coordinated arene resonances observed in the ^1H NMR spectra. On stand-

(37) Fagan, P. J.; Ward, M. D.; Calabrese, J. C. *J. Am. Chem. Soc.* **1989**, *111*, 1698. Ward, M. D.; Fagan, P. J.; Calabrese, J. C.; Johnson, D. C. *J. Am. Chem. Soc.* **1989**, *111*, 1719.

(38) Gemel, C.; Kirchner, K.; Schmid, R.; Mereiter, K. *Organometallics* **1996**, *15*, 532. Kriesel, J. W.; Konig, S.; Freitas, M. A.; Marshall, A. G.; Leary, J. A.; Tilley, T. D. *J. Am. Chem. Soc.* **1998**, *120*, 12207.

(39) Khaleel, A.; Klabunde, K. J. *Inorg. Chem.* **1996**, *35*, 3223. Jagirdar, B. R.; Palmer, R.; Klabunde, K. J.; Radonovich, L. J. *Inorg. Chem.* **1995**, *34*, 278. Prout, K.; Gourdon, A.; Couldwell, C.; Meunier, B.; Miao, F. M.; Woolcock, J. *Acta Crystallogr., Sect. B* **1982**, *38*, 456. Batsanov, A. S.; Struchkov, Yu. T.; Zaitseva, N. N.; Yur'eva, L. P.; Kravtsov, D. N. *Metalloorg. Khim. (Organomet. Chem. USSR)* **1989**, *2*, 586.

(40) Luo, L.; Nolan, S. P. *Organometallics* **1994**, *13*, 4781.

(41) de los Ríos, I.; Jiménez-Tenorio, M.; Padilla, J.; Puerta, M. C.; Valerga, P. *Organometallics* **1996**, *15*, 4565.

(42) Uson, R.; Oro, L. A.; Ciriano, M. A.; Naval, M. M.; Apreda, M. C.; Foces-Foces, C.; Cano. F. H.; García-Blanco, S. *J. Organomet. Chem.* **1983**, *256*, 331.

(43) Jia, G.; Ng, W. S.; Chu, H. S.; Wong, W.-T.; Yu, N.-T.; Williams, I. D. *Organometallics* **1999**, *18*, 3597.

Scheme 1. Reaction Sequence for the Formation and Degradation of Compounds 7 and 8

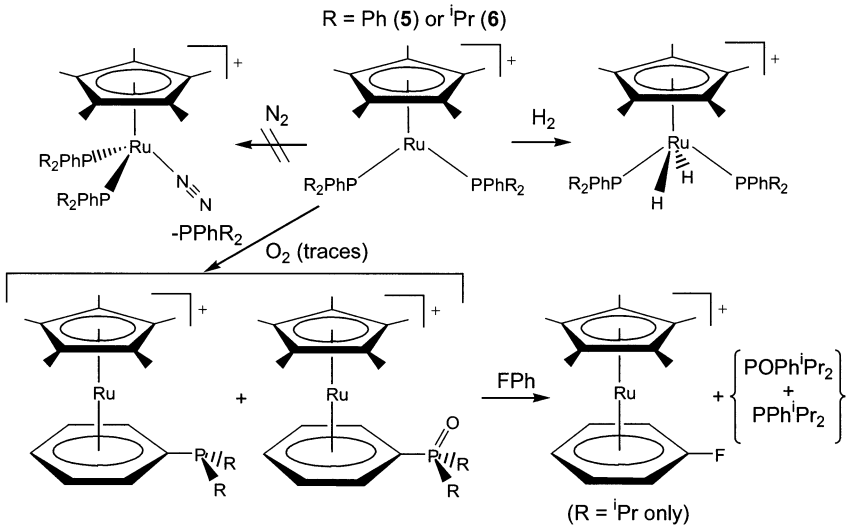

Table 2. Experimental and Optimized Structural Data for Various $[RuCpL_2]^+$ Complexes[a]

$[(C_5R_5)RuL_2]^+$	av M−C_5 (Å)	M−L (Å)	L−M−L (deg)	α (deg)[a]
		$[CpRu(NN)]^+$ Complexes		
$[CpRu(H_2NCH_2CH_2NH_2)]^+$	2.165	2.218, 2.217	78	171
$[CpRu(NH_3)_2]^+$	2.196	2.202, 2.192	91	179
$[CpRu(Me_2NCH_2CH_2NMe_2)]^+$	2.09(1)	2.142(6), 2.163(8)	80.9(1)	180
$[Cp^*Ru(Me_2NCH_2CH_2NMe_2)]^+$	2.142(7)	2.183(7), 2.180(6)	80.3(3)	179
$[Cp^*Ru(Me_2NCH_2CH_2N(Bu^i)_2)]^+$	2.13(1)	2.18(1), 2.21(1)	78.1(5)	168
		$[CpRu(PP)]^+$ Complexes		
$[CpRu(H_2PCH_2CH_2PH_2)]^+$	2.248	2.346	83	149
$[CpRu(PH_3)_2]^+$	2.241	2.355, 2.357	96	152
$[Cp^*Ru(PEt_3)_2]^+$	2.201	2.275, 2.355	99.3	170
$[Cp^*Ru(dippe)]^+$	2.206(3)	2.331(1), 2.356(1)	83.13(4)	160
$[RuCp^*(PMePr^i_2)_2]^+$	2.182(5)	2.393(1), 2.395(1)	101.4(1)	171

[a] α = C_5 ring(centroid)−Ru−L_2(centroid).

ing in fluorobenzene, $[Cp^*Ru(PPh^iPr_2)_2][BAr'_4]$ converted to mixtures of $[Cp^*Ru(\eta^6\text{-}C_6H_5P^iPr_2)][BAr'_4]$ and $[Cp^*Ru(\eta^6\text{-}C_6H_5PO^iPr_2)][BAr'_4]$ and finally yielded $[Cp^*Ru(\eta^6\text{-}C_6H_5F)][BAr'_4]$ (**4**) plus variable relative amounts of free PPh^iPr_2 and $POPh^iPr_2$ (Scheme 1). This process is not observed in the case of the PPh_3 derivatives under otherwise identical conditions.

In summation, all coordinatively unsaturated ruthenium phosphine half-sandwich complexes considered here have bent or pseudo-bent (pseudo-C_{2v}) geometries, with the pyramidal distortion depending on the size of the phosphine. The free space available through bending allows agostic interactions to occur between the alkyl hydrogens and the ruthenium center. Thereby the coordinatively unsaturated character is partially compensated. In contrast, there is no agostic interaction in the pseudo-planar complex $[Cp^*Ru(PMe^iPr_2)_2]^+$. Thus, bending actually activates the metal acceptor ability. The ground-state structures of model 16e complexes $[CpRu(EH_3)_2]^+$ and $[CpRu(H_2ECH_2CH_2EH_2)]^+$, where E = P, N, have been determined by means of DFT calculations. Table 2 summarizes the results of the DFT-optimized geometries, revealing that they are in good agreement with comparable experimental data. Relative B3LYP energies of optimized $[CpRu(H_2ECH_2CH_2EH_2)]^+$ at various angles α = Cp(centroid)−Ru−L_2(centroid) are depicted in Figure 4. The ground-state structure of the phosphine complex is strongly pyramidalized, with α = 149° close to the ideal pseudo-octahedral ML_5 coordination, and the energy differing by about 6 kcal/mol between the ideally planar (180°) and the pyramidal (149°) geometry. In contrast, the related amine complexes adopt the C_{2v} structure. The optimized geometry of $[CpRu(H_2NCH_2CH_2NH_2)]^+$ is close to the experimental molecular structures of $[Cp^*Ru(Me_2NCH_2CH_2NR_2)]^+$ (R = Me, ^{i}Bu)[18] and $[CpRu(Me_2NCH_2CH_2NMe_2)]^+$,[17] the angle α varying from 168 to 180°. In other words, amine ligands participate much less in the LUMO than phosphine ligands. This participation in the LUMO is further increased on bending. However, bending is hampered by bulky L_2 ligands, and the reactivity is modified accordingly.

The reactivity of the unsaturated $CpML_2$ complexes is, of course, mainly given by their acceptor propensity, which in turn depend on the energy and the spatial orientation of the LUMO. This feature is reflected by the agostic interaction between the hydrogen atoms of an isopropyl group and ruthenium in $[Cp^*Ru(dippe)]^+$ or the addition of σ-donors, such as dinitrogen and PR_3. Furthermore, the combination of the σ-accepting and π-donating properties of $Cp'ML_2$ creates the conditions for the η^2-mode addition of not only unsaturated compounds but also the simple σ-bond of dihydrogen.

It may be mentioned that even the Ru−C_5 distances as well as the ^{13}C NMR resonances of the ring carbon atoms of the Cp* ligand can be used as criteria to distinguish preliminarily between 16e and 18e complexes, as shown in Figure 5.

Reactivity of the 16e Complexes. Before, the reactivity of $[Cp^*Ru(PEt_3)_2]^+$ [23,26,44] and $[Cp^*Ru$-

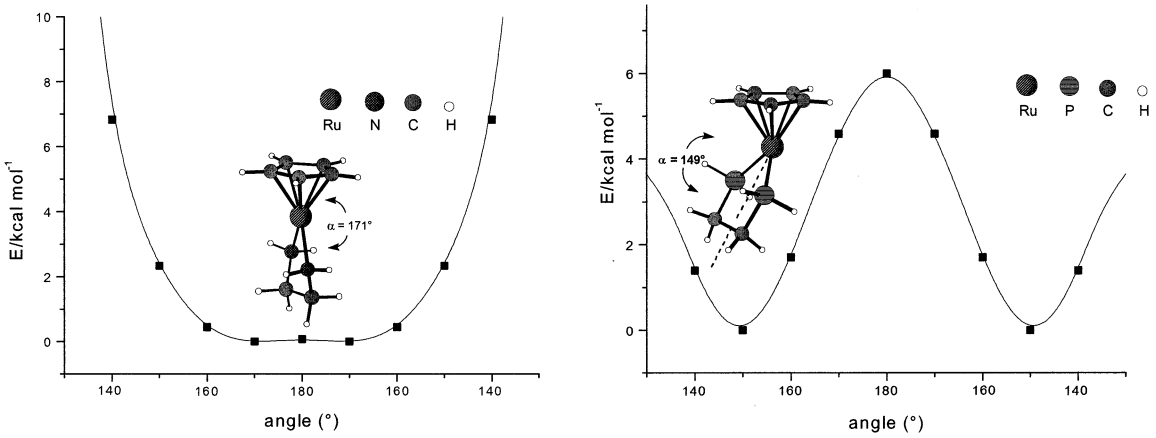

Figure 4. B3LYP energies of optimized $[CpRu(H_2NCH_2CH_2NH_2)]^+$ and $[CpRu(H_2PCH_2CH_2PH_2)]^+$ at various angles α = Cp(centroid)−Ru−L_2(centroid).

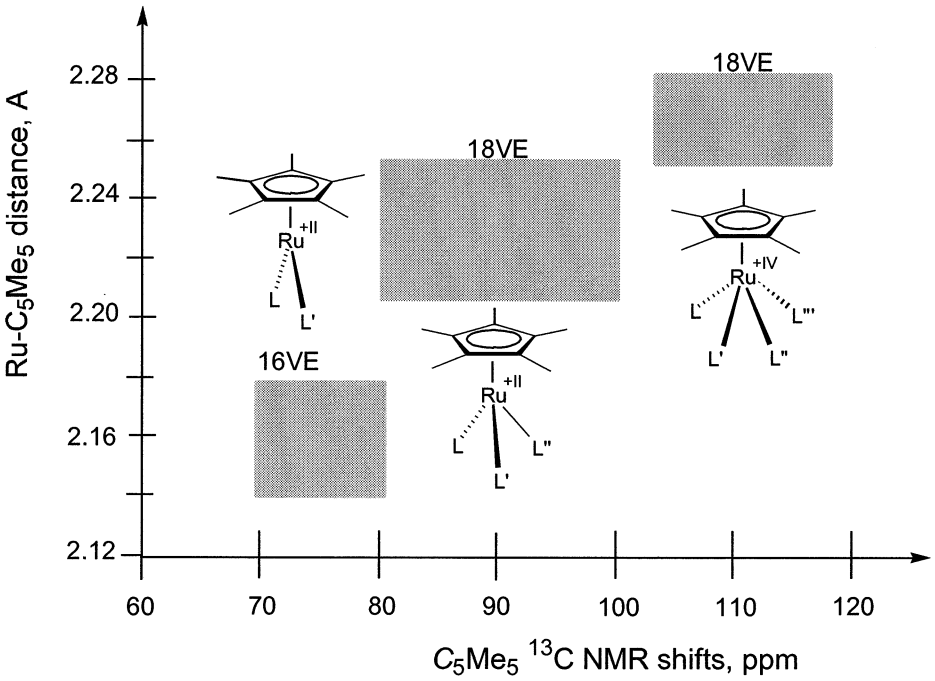

Figure 5. Relationship between Ru−Cp* bond distances and the ^{13}C NMR resonances of the ring carbon atoms of the Cp* ligand in Cp*RuL_n complexes.

(dippe)]$^+$ [25,41,45−47] was explored in situ by starting from suitable 18e precursors containing labile ligands. Now, the complexes **1**−**3** as well as **5** and **6** offer the opportunity to carry out direct experimental studies on the binding and activation of substrates by a coordinatively unsaturated ruthenium center. The transformation into the 18e configuration can be attained in three different ways, namely (a) direct ligand addition, (b) oxidative addition, and (c) degradation to other stable 18e species. Scheme 2 summarizes the reactivity of compounds **1**−**3**. It is worth noting that these complexes exhibit different degrees of affinity for an additional ligand.

Reaction with N_2. When exposed to a dinitrogen atmosphere, both **1** and **2** form the respective dinitrogen complexes $[Cp^*Ru(N_2)(PEt_3)_2]^+$ and $[Cp^*Ru(N_2)(dippe)]^+$, which were characterized previously in the form of their $[BPh_4]^-$ salts.[23,41] In contrast, **3** is unreactive toward dinitrogen, and so is **5** and **6** (Schemes 1 and 2).

Reaction with PR_3. Complex **1** reacts with an excess of phosphine to yield the 18e tris(phosphine) derivative $[Cp^*Ru(PEt_3)_3][BAr'_4]$ (**7**). An ORTEP view of **7** is presented in Figure 6, showing a three-legged piano-stool structure with the three phosphine ligands in a *fac* disposition around ruthenium and slightly elongated Ru−Cp* separations. This structure is very similar to that of the cation of $[CpRu(PMe^iPr_2)_3][BAr'_4]$, recently reported by us.[21] Thus, the ease of PEt_3 dissociation provides a pathway for the stabilization of electrophilic

(44) Bustelo, E.; Jiménez-Tenorio, M.; Puerta, M. C.; Valerga, P. *Organometallics* **1999**, *18*, 4563.
(45) de los Ríos, I.; Jiménez-Tenorio, M.; Puerta, M. C.; Valerga, P. *J. Am. Chem. Soc.* **1997**, *119*, 652.
(46) Coto, A.; de los Ríos, I.; Jiménez-Tenorio, M.; Puerta, M. C.; Valerga, P. *J. Chem. Soc., Dalton Trans.* **1999**, 4309.
(47) Bustelo, E.; Jiménez-Tenorio, M.; Puerta, M. C.; Valerga, P. *Eur. J. Inorg. Chem.* **2001**, 2391. Bustelo, E.; Jiménez-Tenorio, M.; Puerta, M. C.; Valerga, P.; Mereiter, K. *Organometallics* **2002**, *21*, 1903.
(48) Gemel, C.; LaPensee, A.; Mauthner, K.; Mereiter, K.; Schmid, R.; Kirchner, K. *Monatsh. Chem.* **1997**, *128*, 1189.
(49) Mauthner, K.; Mereiter, K.; Schmid, R.; Kirchner, K. *Inorg. Chim. Acta* **1995**, *236*, 95. Kirchner, K.; Mauthner, K.; Mereiter, K.; Schmid, R. *J. Chem. Soc., Chem. Commun.* **1993**, 892.

Scheme 2. Summary of the Reactivity of Compounds 1−3

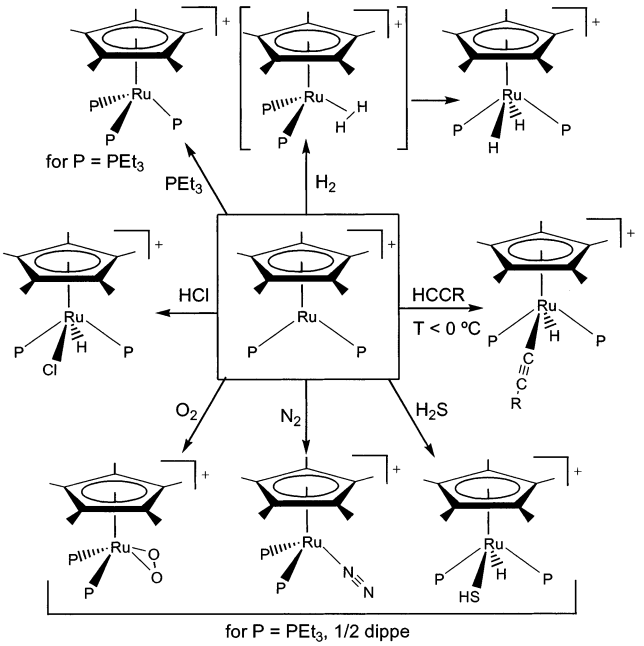

species. This feature has already been noted in the context of the formation of the zwitterionic alkynylphosphonio species $[Cp^*Ru\{C{\equiv}CC(PEt_3)Me_2\}(PEt_3)_2][BPh_4]$, resulting from nucleophilic attack of PEt_3 at the γ-carbon of the highly electrophilic allenylidene derivative $[Cp^*Ru\{{=}C{=}C{=}CMe_2\}(PEt_3)_2][BPh_4]$. In this case no external source of PEt_3 is required.[44] A similar behavior was observed in connection with halide abstraction from $[Cp^*RuCl(PMe_3)_2]$, giving a mixture of **4** and the tris(phosphine) derivative $[Cp^*Ru(PMe_3)_3][BAr'_4]$ (**8**), as mentioned above. With an excess of phosphine the compounds **3**, **5**, and **6** do not transform into the 18e tris(phosphine) derivatives of the type $[Cp^*Ru(PR_3)_3]^+$.

Reaction with O_2. All compounds (**1**−**3**, **5**, and **6**) react with oxygen, but in different ways. The species **1** and **2** bind O_2 irreversibly, furnishing the dioxygen complexes $[Cp^*Ru(O_2)(PEt_3)_2]^+$[26] and $[Cp^*Ru(O_2)(dippe)]^+$,[25] which were isolated previously and characterized as the $[BPh_4]^-$ salts. Exposure of solutions of **5** and **6** to oxygen, on the other hand, causes rapid decomposition of the complex with concomitant formation of the respective phosphine oxides $POPh_3$ and $POPh^iPr_2$. As shown in Scheme 1, the phosphine oxides bind to the Cp*Ru moieties in an η^6 fashion, furnishing the cationic sandwich complexes $[Cp^*Ru(\eta^6\text{-}C_6H_5POR_2)][BAr'_4]$ (R = Ph (**5b**), ^{i}Pr (**6b**)). Fluorobenzene and dichloromethane solutions of **3** gradually turn red-brown when exposed to air. NMR monitoring (in CD_2Cl_2) indicates a slow formation of paramagnetic species, with no evidence of formation of a diamagnetic dioxygen complex: i.e., $[Cp^*Ru(O_2)(PMe^iPr_2)_2][BAr'_4]$. Attempts to isolate the reaction product failed—a brown oil was the only result. Trying to use another anion, we treated a solution of **3** in MeOH in the air with an excess of $NaBPh_4$. After a few minutes, a crystalline precipitate was formed, which upon isolation turned out to be the sandwich derivative $[Cp^*Ru(\eta^6\text{-}C_6H_5BPh_3)]$.[48] Thus, the nature of the product of the interaction of **3** with dioxygen remains unknown. It can be stated though that the reactivity pattern of this compound toward O_2 does not match that of its congeners **1** and **2** or other Cp*Ru moieties capable of forming stable dioxygen complexes, such as $[Cp^*Ru(O_2)(dppm)]^+$[43] and $[Cp^*Ru(O_2)(dppe)]^+$.[49]

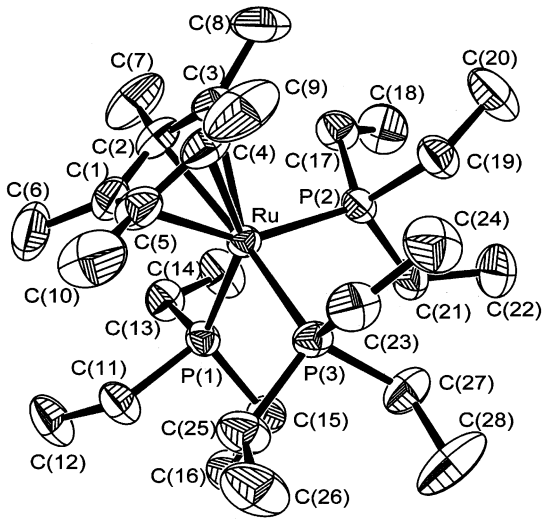

Figure 6. ORTEP drawing (50% thermal ellipsoids) of the cation $[Cp^*Ru(PEt_3)_3]^+$ in complex **7**. Hydrogen atoms have been omitted. Selected bond lengths (Å) and angles (deg) with estimated standard deviations in parentheses: Ru−C(1), 2.290(3); Ru−C(2), 2.283(3); Ru−C(3), 2.301(3); Ru−C(4), 2.286(3); Ru−C(5), 2.270(3); Ru−P(1), 2.353(1); Ru−P(2), 2.354(1); Ru−P(3), 2.355(1); P(1)−Ru−P(2), 96.84(3); P(1)−Ru−P(3), 93.42(3); P(2)−Ru−P(3), 94.74(3).

Reaction with H_2. The reactivity of the $[(C_5R_5)Ru(PP)]^+$ systems toward dihydrogen has been the subject of very detailed studies.[27,41,50−52] The coordinatively unsaturated complexes undergo oxidative addition of H_2, yielding the ruthenium(IV) dihydride complexes $[(C_5R_5)RuH_2(PP)]^+$, which in some instances have been shown to exist in equilibrium with their dihydrogen tautomers $[(C_5R_5)Ru(H_2)(PP)]^+$. Metastable dihydrogen complexes are also generated by protonation of neutral monohydrides at low temperature and, in most cases, rearrange irreversibly to their dihydride tautomers upon raising the temperature. Thus, the reaction of H_2 with $[CpRu(PH_3)_2]^+$ is calculated to be exothermic by 21.9 kcal/mol, respectively. In the dihydrogen complexes, back-donation via d→$\sigma^*(H_2)$ electron transfer is strong and, therefore, the rotation of the η^2-H_2 ligand is hindered. Lowering the $\sigma^*(H_2)$ orbital energy can ultimately complete the electron transfer to H_2 toward oxidative addition, giving the classic Ru(IV) dihydride complexes. According to the DFT calculations both η^2-dihydrogen and classical dihydride complexes $[CpRu(PH_3)_2(\eta^2\text{-}H_2)]^+$ and *trans*-$[CpRu(PH_3)_2(H)_2]^+$ as well as $[CpRu(H_2PCH_2CH_2PH_2)(\eta^2\text{-}H_2)]^+$ and $[CpRu(H_2PCH_2CH_2PH_2)(H)_2]^+$ are stable systems differing only slightly in energy (Figure 7). While in the case of the monodentate system the dihydride species is more stable by

(50) (a) Jia, G.; Lau, C. P. *J. Organomet. Chem.* **1998**, *565*, 37. (b) Gelabert, R.; Moreno, M.; Lluch, J. M.; Lledós, A. *J. Am. Chem. Soc.* **1997**, *119*, 9840. (c) Chinn, M. S.; Heinekey, D. M. *J. Am. Chem. Soc.* **1990**, *112*, 5166.

(51) Klooster, W. T.; Koetzle, T. F.; Jia, G.; Fong, T. P.; Morris, R. H.; Albinati, A. *J. Am. Chem. Soc.* **1994**, *116*, 7677. Jia, G.; Lough, A. J.; Morris, R. H. *Organometallics* **1992**, *11*, 161. Jia, G.; Morris, R. H. *J. Am. Chem. Soc.* **1991**, *113*, 875.

(52) Brammer, L.; Klooster, W. T.; Lemke, F. R. *Organometallics* **1996**, *15*, 1721.

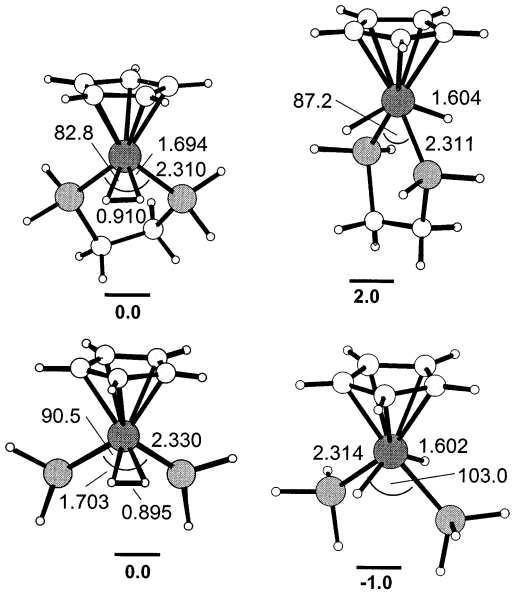

Figure 7. B3LYP energies (kcal mol^{-1}) of optimized dihydrogen and *trans*-dihydride complexes of $[CpRu(PH_3)_2]^+$ and $[CpRu(H_2PCH_2CH_2PH_2)]^+$.

merely 1.0 kcal/mol, the situation is reversed for the chelate complex, where the dihydrogen complex is more stable by 2.0 kcal/mol. It is interesting to note that similar results have been found for the related complexes $[CpRu(H_2PCH_2PH_2)(\eta^2\text{-}H_2)]^+$ and $[CpRu(H_2PCH_2PH_2)(H)_2]^+$, where the first complex is slightly more stable.[50b] This is in line with the experimental findings that frequently both dihydrogen and *trans*-dihydride Ru(IV) complexes can be observed in solution, at least at lower temperatures. Attempts to optimize the geometry of the *cis*-dihydride complex failed, resulting in collapse of the structure to afford the dihydrogen complex. This finding is in line with the fact that, to date, no *cis*-dihydride complexes of the type $[CpRu(PP)(H)_2]^+$ have been isolated or spectroscopically detected. Furthermore, it is interesting to note that we were unable to locate a transition state directly connecting the dihydrogen and the *trans*-dihydride complex.

For the systems in our hands both dihydride $[Cp^*RuH_2(PP)]^+$ and dihydrogen $[Cp^*Ru(H_2)(PP)]^+$ complexes have previously been identified where PP = $(PEt_3)_2$,[26] dippe,[41] $(PPh_3)_2$.[50,51] All of the dihydride structures have the transoid configuration.

The reaction of **3** with H_2 in CD_2Cl_2 at −80 °C yielded exclusively the dihydride complex $[Cp^*RuH_2(PMe^iPr_2)_2]^+$.[26] The same product resulted from the protonation of $[Cp^*RuH(PMe^iPr_2)_2]$ with HBF_4 at −80 °C, whereas the dihydrogen tautomer $[Cp^*Ru(H_2)(PMe^i$-

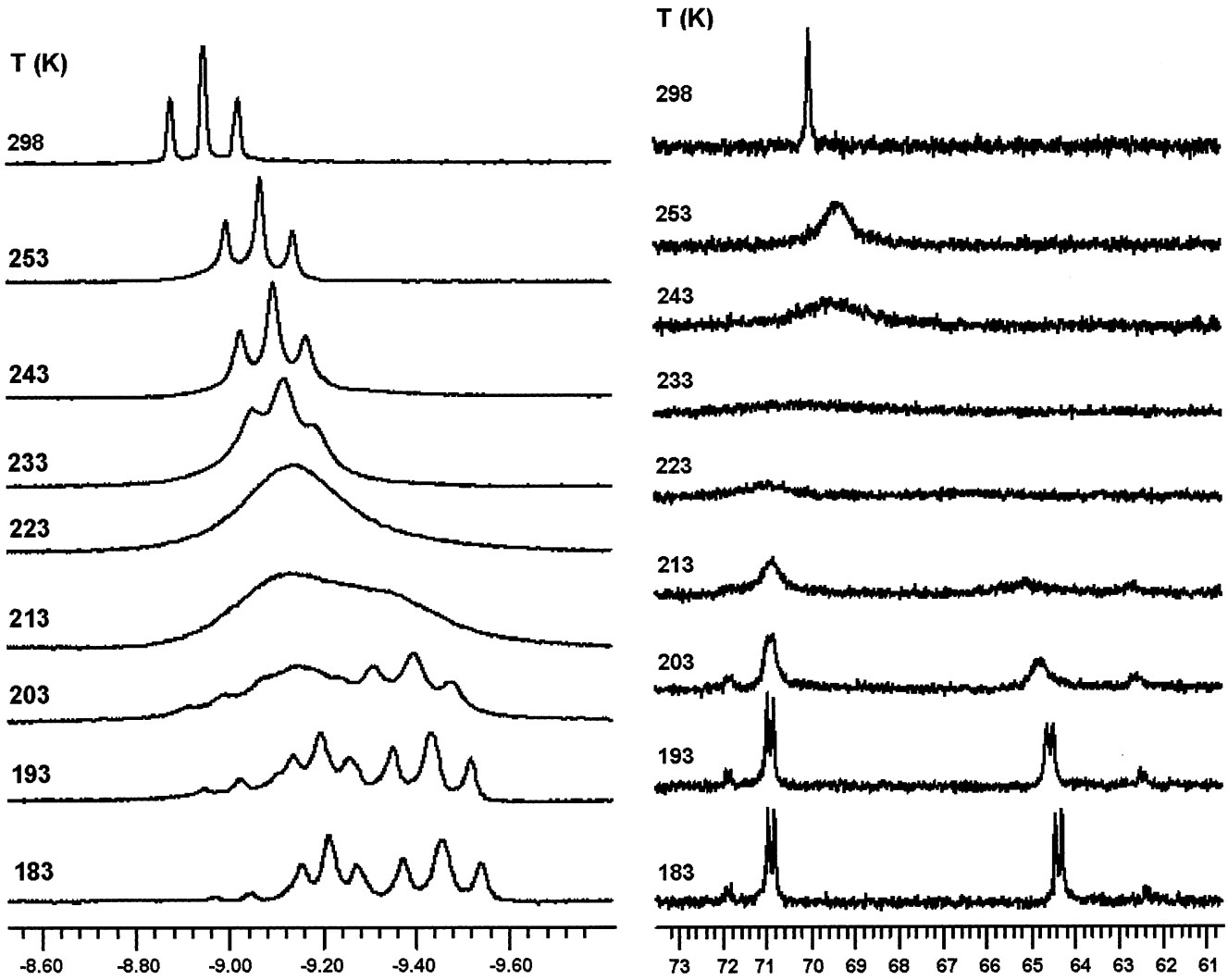

Figure 8. Variable-temperature ^1H (hydride region) and $^{31}P\{^1H\}$ NMR spectra (CD_2Cl_2) of the dihydride complex **9**.

Chart 1

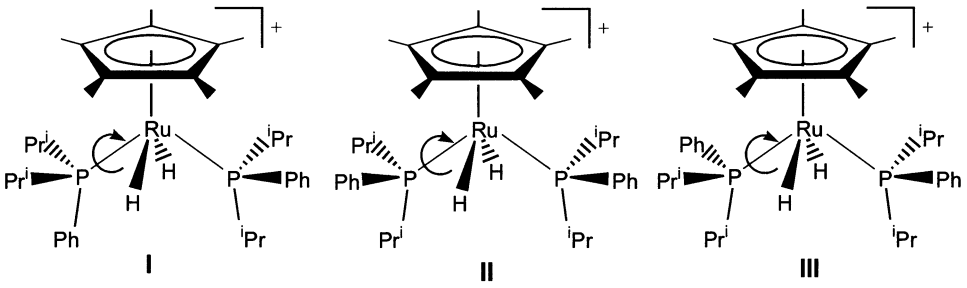

$Pr_2)_2]^+$ was not detected. In an analogous fashion, the dihydride complex $[Cp^*RuH_2(PPh^iPr_2)_2][BAr'_4]$ (**9**) was obtained either by reaction of $[Cp^*RuCl(PPh^iPr_2)]$ with H_2 and $NaBAr'_4$ in FPh in the presence of PPh^iPr_2 or by protonation of the monohydride $[Cp^*RuH(PPh^iPr_2)_2]$ (**10**) at low temperature, with no evidence for the presence of the dihydrogen isomer $[Cp^*Ru(H_2)(PPh^iPr_2)_2][BAr'_4]$.

The NMR spectra of **9** are found to change with temperature (Figure 8). The hydride resonance appears as one triplet in the ^1H NMR spectrum at room temperature. This signal broadens when the temperature is lowered. Below 213 K, it decoalesces to several triplet signals. The $^{31}P\{^1H\}$ NMR spectrum consists of one singlet at room temperature but becomes featureless at 233 K, and new sets of resonances appear below 213 K. These sets correspond to two AM spin systems, in the ratio 83:17 in CD_2Cl_2 at 193 K. The $(T_1)_{min}$ values between 450 and 600 ms (CD_3COCD_3, 400 MHz, 183 K) for the hydride resonances indicate a classical dihydride structure for **9**. These features can be rationalized by assuming an equilibrium between rotamers of the phosphine in a transoid dihydride. For each rotational isomer, one group on each phosphine is pointing away from Cp*, and the other two are to the sides; hence, several possible rotamers are possible, as shown in Chart 1.

From NMR spectroscopy, it seems that there is one major species having two inequivalent hydrides (each a doublet of doublets of doublets with $^2J(H,P_A)$, $^2J(H,P_M)$, and a small $^2J(H,H')$) and inequivalent phosphorus. This rotamer may well have one Ph and one ^{i}Pr pointing away from the Cp* (rotamer **I**), since the other combinations (rotamers **II** and **III**) would have equivalent phosphorus atoms. There is another minor rotamer with inequivalent phosphorus atoms, associated with the triplet at −9.03 ppm in the ^1H NMR spectrum, although another hydride multiplet corresponding to this rotamer could be hidden in the hydride signal of the major isomer. For this rotamer we can think of an arrangement of phosphines in an alternated disposition, one with the phenyl group pointing away from the Cp* and another one with one Ph substituent pointing toward the Cp* (i.e., like the disposition of PMe^iPr_2 found in the X-ray structure of **3**). Therefore, possible structures of the rotamers observed at low temperature consistent with NMR data should be those shown in Scheme 3.

The X-ray crystal structure of **9** was determined with an ORTEP view of the complex cation shown in Figure 9. Consistent with the NMR data, the cation shows a four-legged piano-stool structure with the hydrides in a transoid disposition. The phosphine ligands are inequivalent, due to the orientations of the phenyl substituents, with a torsion angle C(11)−P(1)−P(2)−C(23) of 83.9°. The plane P(1)−Ru−P(2) is almost perpendicular (87.3°) to the plane defined by the C_5 ring of the Cp*. The Ru−H(1Ru) and Ru−H(2Ru) separations of 1.50(3) and 1.53(3) Å compare well with the values of 1.599(8) and 1.604(9) Å obtained from the Ru−H bond lengths in $[Cp^*RuH_2(PMe_3)_2][BF_4]$.[52] Likewise, the H(1Ru)−Ru−H(2Ru) and P(1)−Ru−P(2) angles of 124.5(17) and 107.96(2)°, respectively, are close to those in $[Cp^*RuH_2(PMe_3)_2][BF_4]$ (118.8(4) and 111.1(2)°).[52] Therefore, the X-ray structure is consistent with that of rotamer **I**; the minor species observed in solution by NMR spectroscopy may have slightly different orientations of the phenyl groups resulting from the different torsion angle C(11)−

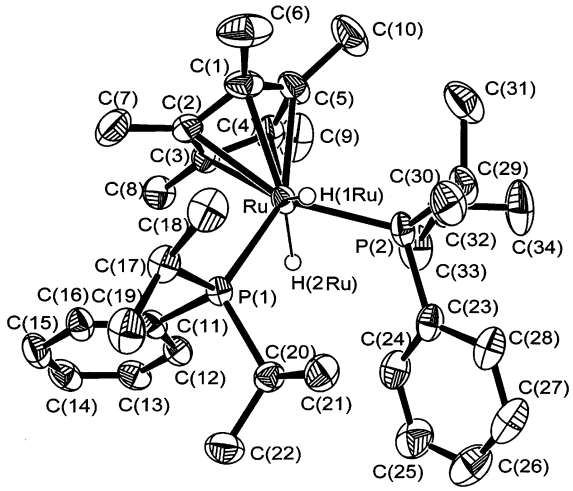

Figure 9. ORTEP drawing (50% thermal ellipsoids) of the cation $[Cp^*RuH_2(PPh^iPr_2)_2]^+$ in complex **9**. Hydrogen atoms, except hydrides, have been omitted. Selected bond lengths (Å) and angles (deg) with estimated standard deviations in parentheses: Ru−H(1Ru), 1.50(3); Ru−H(2Ru), 1.53(3); Ru−C(3), 2.255(2); Ru−C(4), 2.266(2); Ru−C(2), 2.294(2); Ru−C(1), 2.309(2); Ru−C(5), 2.314(2); Ru−P(1), 2.3454(7); Ru−P(2), 2.3514(7); H(1Ru)−Ru−H(2Ru), 124.5(17); P(1)−Ru−P(2), 107.96(2).

Scheme 3. Proposed Structures for the Rotameric Isomers of Compound 9 in Equilibrium

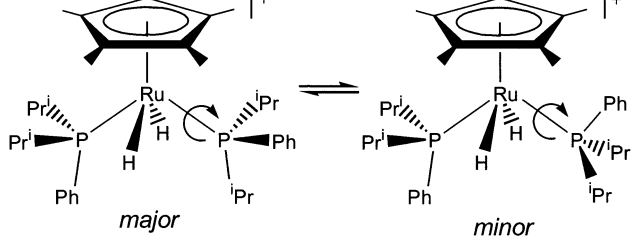

P(1)−P(2)−C(23). Rotation around the Ru−P bonds at higher temperatures causes averaging between all possible rotamers, leading to equivalent hydride and phosphorus atoms. It is interesting to note that the dynamic behavior exhibited by **9** is exceptional, not found with the related dihydride complexes $[Cp^*RuH_2(PMe^iPr_2)_2]^+$ [26] and $[Cp^*RuH_2(PMePh_2)_2]^+$.[51]

Reaction with HCl. The compounds **1**−**3** also undergo oxidative addition of HCl, yielding the ruthenium(IV) chloro hydrido complexes $[Cp^*RuHCl(PEt_3)_2][BAr'_4]$ (**12**), $[Cp^*RuHCl(dippe)][BAr'_4]$ (**13**), and $[Cp^*RuHCl(PMe^iPr_2)_2][BAr'_4]$ (**14**). Whereas **12** and **13** were readily prepared by reaction of **1** or **2** with anhydrous HCl, generated from Me_3SiCl and MeOH in Et_2O, in the case of **3** the dihydride was obtained. However, **14** was accessible by reaction of **3** with aqueous HCl. The reaction of **5** with HCl was not clean, probably due to phosphine dissociation further complicated by the presence of protons. The ^1H NMR spectra of compounds **12**−**14** display one triplet resonance in the hydride region, as expected, whereas the $^{31}P\{^1H\}$ NMR spectra consist of one singlet. No changes were observed on lowering the temperature. Hence, a four-legged piano-stool structure can be proposed for these derivatives. Other molecules such as H_2S and 1-alkynes have been shown to give oxidative addition reactions with the complexes $[Cp^*Ru(PP)]^+$ (PP = $(PEt_3)_2$, dippe), yielding the ruthenium(IV) hydrido metallothiol $[Cp^*RuH(SH)(PP)]^+$ [25,48] and hydrido alkynyl derivatives $[Cp^*RuH(C{\equiv}CR)(PP)]^+$.[46,47,49] We have found that the reaction of **3** with 1-alkynes also leads to the hydrido alkynyl complex $[Cp^*RuH(C{\equiv}CR)(PMe^iPr_2)_2][BAr'_4]$. The structure, dynamics, and reactions of these species will be described in detail in a forthcoming paper.

In summation, the properties of the coordinatively unsaturated $[CpRu(PP)]^+$ complexes appear to be connected with the ease of bending of the ligands, since species with bulky and rigid ligands are relatively inert. Thus, the complexes **1** and **2** easily form 18e adducts with σ-ligands, such as N_2 and PR_3, in contrast to complex **3**, most likely due to van der Waals repulsions between Cp* and the PMe^iPr_2 pieces. Actually, interligand interactions are being increasingly recognized as an important factor in determining the coordination geometry and reactivity of many metal complexes.[53]

Acknowledgment. We thank the Ministerio de Educación y Cultura of Spain (DGICYT, Project BQU-2001-4046, Accion Integrada HU-2001-0020) for financial support, Johnson Matthey plc for generous loans of ruthenium trichloride, and the Royal Society of Chemistry for the award of a grant for international authors (to M.J.T.). Suggestions from Prof. Robert H. Morris, University of Ontario (Toronto, Canada), are also gratefully acknowledged.

Supporting Information Available: Tables of X-ray structural data, including data collection parameters, positional and thermal parameters, and bond distances and angles, for complexes **1**−**4**, **7**, and **9**. This material is available free of charge via the Internet at http://pubs.acs.org.

OM020359R

(53) Sapunov, V. N.; Kirchner, K.; Schmid, R. *Coord. Chem. Rev.* **2001**, *214*, 143.